

Geology, geochronology and geochemistry of the 2.05 Ga gneissic A1-type granites and related intermediate rocks in central Finland: implication for the tectonic evolution of the Karelia craton margin



KIMMO KÄRENLAMPPI^{1*}, ASKO KONTINEN², HANNU HUHMA³
AND EERO HANSKI¹

¹ *Oulu Mining School, University of Oulu, P.O. Box 3000, 90014 Oulu, Finland*

² *Geological Survey of Finland, P.O. Box 1237, 70211 Kuopio, Finland*

³ *Geological Survey of Finland, P.O. Box 96, 02151 Espoo, Finland*

Abstract

The 2.05 Ga Otanmäki suite represents a globally rare occurrence of Paleoproterozoic non-orogenic A1-type magmatism. It consists of a broad variety of A-type felsic and intermediate igneous rocks including monzodiorites, monzonites, syenites and peralkaline to peraluminous granites, containing both plutonic and subvolcanic members. The suite has chemical characteristics similar to those of A1-type suites formed in intraplate hotspots or continental rifts by differentiation of variably crustally contaminated, mafic mantle-derived magmas. However, compared to the Otanmäki rocks, most A1-type suites are considerably younger.

Unraveling the original geologic setting of the Otanmäki suite is challenging because the suite was disintegrated, deformed and metamorphosed under amphibolite facies conditions (T ~550–600 °C, P ~4 kbar) during the Svecofennian collisional orogeny (ca. 1900 Ma), i.e., 150–200 Ma after its initial emplacement. As a result, Otanmäki suite rocks are now found as pervasively foliated rocks within two nappe units sandwiched between Archean granitoid gneiss complexes and Paleoproterozoic supracrustal belts. The occurrence of slivers of 1950 Ma ocean-continent-transition ophiolitic rocks in the same thrust belt and the proximity of the Otanmäki suite to the Karelia-Svecofennia margin suggest that the suite records an early stage of a slow, ca. 100-Ma-long extension-rifting process which, at ca. 1950 Ma, eventually led to the final break-up of the Karelia craton and formation of the nascent ocean basin witnessed by the Jormua ophiolite complex.

Keywords: A1-type granite, petrogenesis, continental rifting, Karelia craton, Paleoproterozoic, Finland

*Corresponding author (e-mail: kimmo.karenlampi@oulu.fi)

Editorial handling: Jussi S. Heinonen (jussi.s.heinonen@helsinki.fi)

1. Introduction

The Proterozoic granitoid magmatism in Finland is dominated by Svecofennian pre-, syn- and postorogenic plutonism, which took place in the time interval of 1.93–1.77 Ga (Nironen, 2005), and subsequent 1.64–1.54 Ga non-orogenic A-type rapakivi granites (Rämö & Haapala, 2005). Before 1.93 Ga, the Paleoproterozoic geological evolution involved mostly deposition of Karelian sedimentary rocks and mafic and minor felsic volcanic rocks on the Archean basement and emplacement of coeval mafic intrusions, but with only minimal felsic plutonism (Laajoki, 2005; Iljina & Hanski, 2005; Vuollo & Huhma, 2005; Hanski, 2013; Hanski & Melezhik, 2013a,b). However, there are some relatively small granitic plutons in northern and eastern Finland, which have yielded older Paleoproterozoic ages, such as 2.4 Ga (Mikkola, 2011), 2.1 Ga (Ahtonen et al., 2007) and 2.0 Ga (Ranta et al., 2015). These also include the ca. 2.05 Ga Otanmäki suite alkaline granites in central Finland (Fig. 1) (Pääkkönen, 1956; Marmo et al., 1966; Kontinen et al., 2013a), which represent an uncommon occurrence of granitic rocks without any clear counterpart elsewhere in the Fennoscandian Shield. These granites contain rare earth element mineralization (Kärenlampi et al., 2017) and are spatially associated with ca. 2.06 Ga gabbroic intrusions hosting Fe-Ti-V oxide ore deposits (Kuivasaari et al., 2012; Huhma et al., 2018).

Since the first reports in the 1950s and 1960s (Pääkkönen, 1956; Marmo et al., 1966), the Otanmäki suite has remained poorly studied and documented. In the early accounts, the suite was described as consisting of alkaline granites restricted to the Otanmäki area, but in this paper, we present new field and whole-rock geochemical evidence showing that the suite is lithologically much more complex and extends over a much larger area than previously thought, consisting of a spectrum of A-type granites and associated intermediate rocks. We provide the first detailed geological, geochemical and geochronological study of this

globally uncommon occurrence of 2.05 Ga A1-type magmatism. We characterize the main rock types, describe their areal distribution and contact relationships and present new zircon and titanite U-Pb isotope data to better constrain the age of the magmatism. We also discuss the implications of the collected data for the geotectonic environment of the Otanmäki suite, including their potential relationship to the break-up of the Karelia craton. The study will also provide foundation for a follow-up publication focusing in a greater detail on the petrogenesis of the Otanmäki suite granites and intermediate rocks.

2. Geologic setting

The Otanmäki suite A-type granites and related intermediate rocks occur in two tectonic bodies (nappes) at the southwestern margin of the Archean Karelia craton in central Finland, being located 20–75 km to the east of the major tectonic boundary between the Svecofennian island arc collage and the Karelia craton (Fig. 1). The long geological history of the region involves at least four major tectonic stages: 1) Archean orogeny at ca. 2.6–2.7 Ga, 2) a period of cratonization, sedimentation and extensional tectonics between ca. 2.5 and 2.0 Ga, 3) subsequent continental break-up of the Karelia craton between ca. 2.0 and 1.95 Ga, and 4) tectonic reworking in connection with the Svecofennian orogenesis (Laajoki, 2005; Lahtinen et al., 2010, 2015; Hölttä et al., 2012a,b; Hanski & Melezhik, 2013a). The present structural configuration of the area largely reflects the reworking during the Svecofennian collisional orogeny, which initiated at ca. 1.9 Ga and involved several stages of compressional folding and faulting, resulting in burial of the Karelia craton margin under a massive overthrust complex transported from the west-southwest (e.g., Koistinen, 1981; Park, 1985; Gáal, 1990; Tuisku & Laajoki, 1990; Kontinen et al., 1992; Lahtinen et al., 2005, 2015).

The Karelia craton margin is composed mostly of ca. 2.6–2.7 Ga TTG migmatite-gneiss complexes

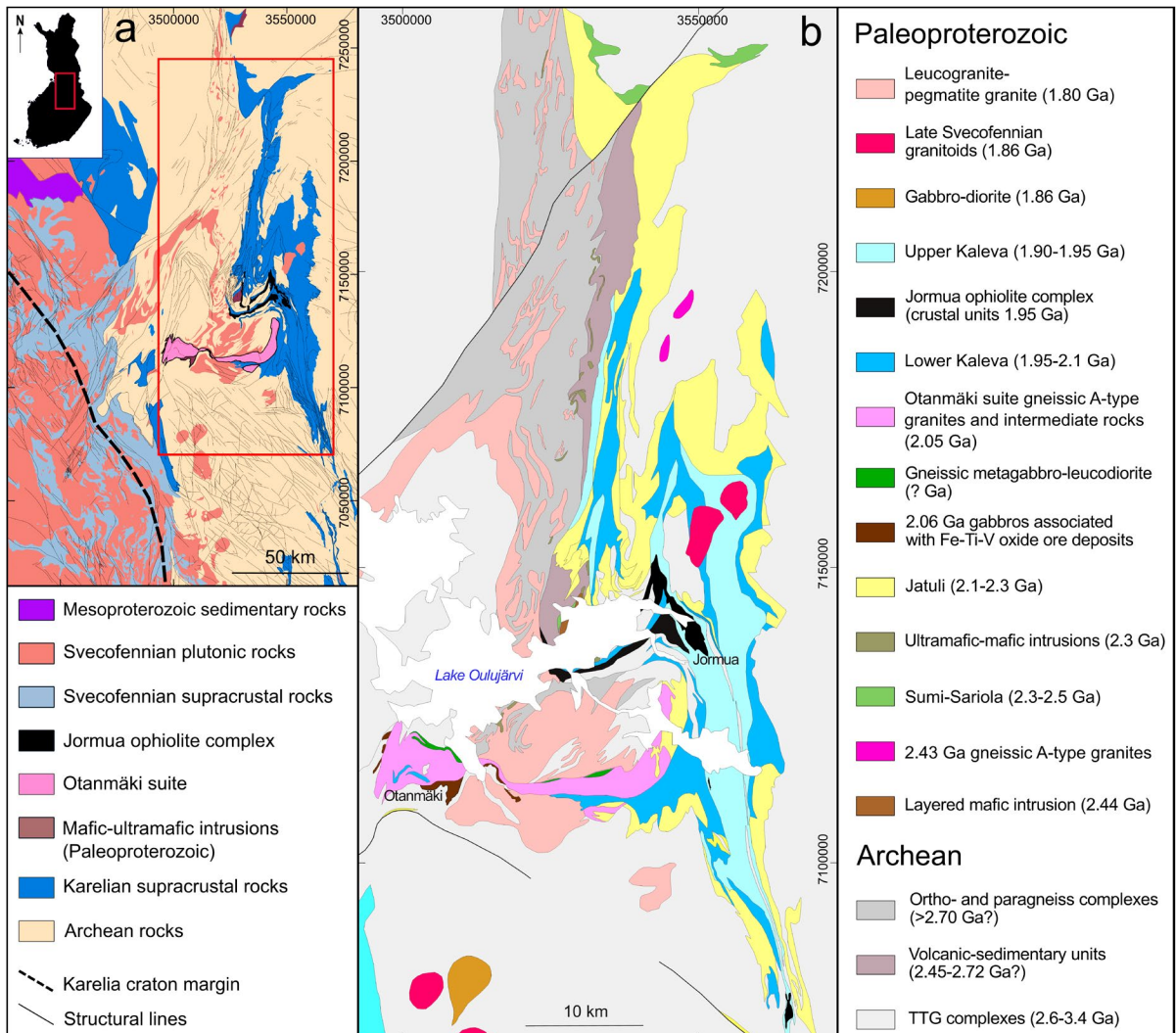


Figure 1. (a) Geological map of central Finland showing the location of the Otanmäki suite nappes close to the inferred buried boundary (dashed line; after Huhma et al., 2011) between the Archean Karelia craton and the Paleoproterozoic Svecofennian domain. The boundaries of rock units are mainly from the Bedrock of Finland 1:200 000 database (<https://hakku.gtk.fi/en>). (b) Geological map of the Kainuu schist belt (modified from Huhma et al., 2018) showing the location of the Otanmäki suite A-type rocks and Jormua ophiolite complex. Coordinates in KKJ-3/Finland Uniform Coordinate System.

and remnants of Paleoproterozoic cover sequences, with the latter being represented by the Karelian formations of the Kainuu schist belt (Vaasjoki et al., 2001; Laajoki, 2005; Hölttä et al., 2012a, b; Kontinen & Hanski, 2015). The supracrustal sequence of the Kainuu schist belt is traditionally divided into three main unconformity-separated units, Sumi-Sariola, Jatuli and Kaleva (Laajoki, 2005; Kontinen & Hanski, 2015). The supracrustal

rocks of the Kainuu schist belt flanking the Otanmäki suite nappes belong to the Jatulian (2.3–2.1 Ga) and Kalevian (2.1–1.9 Ga) formations. The Jatuli consists of cratonic-epicratonic deposits, and the Kaleva includes both rift-phase marine basin deposits (Lower Kaleva) and oceanic basin deposits (Upper Kaleva) (Kontinen & Hanski, 2015). The Jatulian and Lower Kalevian formations represent remnants of autochthonous strata that may have

periodically covered the whole Karelia craton (Jatuli) or parts of it (Lower Kaleva). The thickness of the deformed cover remnants locally reaches several kilometers (Elo, 1997).

The Upper Kaleva metawackes differ from the older, autochthonous sedimentary rocks derived dominantly from Archean sources in having a major Paleoproterozoic (1.92–2.0 Ga) detrital zircon population (Lahtinen et al., 2010; Kontinen & Hanski, 2015). These wackes enclose fragments of mantle and oceanic crust, with the largest of them forming the 1.95 Ga Jormua ophiolite complex located 8–25 km north of the Otanmäki suite nappes (Kontinen, 1987; Peltonen & Kontinen, 2004; Peltonen et al., 2008). The Upper Kaleva sediments and enclosed ophiolites have been interpreted as an allochthonous complex, which was thrust on the Karelia craton margin at ca. 1900 Ma (Kontinen, 1987; Peltonen et al., 2008).

The Archean granitoid gneisses fringing the Otanmäki suite A-type igneous rocks in the western part of the study area host gabbroic intrusions (Fig. 2) that are roughly coeval (ca. 2.06 Ga) with the Otanmäki suite (Huhma et al., 2018). Vanadiferous magnetite-ilmenite deposits in the gabbros were mined from 1953 to 1985 (Lindholm & Anttonen, 1980; Kuivasaari et al., 2012; Sarapää et al., 2015). In addition, two major episodes of late Svecofennian granitic magmatism, at ca. 1.86 and 1.80 Ga, have been identified in the region (Fig. 1). In the study area, the 1.80 Ga event was more significant resulting in dense networks of undeformed pegmatite granite or intermingled medium-grained leucogranite and pegmatite granite dikes, especially in the central part of the study area, but nowhere they form large coherent plutons.

The Svecofennian metamorphic conditions in the study area are estimated to have attained peak temperatures of 550–600 °C and a pressure of about 4.0 kbar (bathograd estimates, garnet-biotite thermometry and garnet-biotite-sillimanite-quartz barometry conducted by us during this study; see Electronic Appendix A). The peak-T conditions are considered to have occurred between ca. 1.87 Ga

and 1.85 Ga, although the heating was protracted, with temperatures falling below ~500 °C only after 1.80 Ga (Kontinen et al., 1992; Peltonen et al., 1996; Tuisku, 1997; Vaasjoki et al., 2001). Blastomylonite textures are characteristic features in sheared rocks of the area, indicating that peak-T conditions were reached under static conditions after the main Svecofennian deformations, which were over before ca. 1.85 Ga (Pajunen & Poutiainen, 1999; Vaasjoki et al., 2001; Kontinen & Paavola, 2006; Kontinen et al., 2013b,c). The most plausible explanation to the observed Svecofennian heating is tectonic burial of the presently exposed rocks to depths of 15–20 km in association with the 1.9–1.8 Ga folding and thrusting event, although igneous underplating could have been an additional factor (Kontinen et al., 1992, 2013b,c; Tuisku, 1997; Korsman et al., 1999; Pajunen & Poutiainen, 1999; Kontinen, 2002; Kontinen & Paavola, 2006; Lahtinen et al., 2010, 2015).

3. Sampling and methods

The field work for this study (2005–2006, 2016–2017) produced about 6500 outcrop observations, which are supplemented with field data gathered earlier by Rautaruukki Oy exploration and the Geological Survey of Finland (GTK). In addition, a total of 21 diamond drillcores available from the Otanmäki area were studied and sampled. In outlining the rock units, airborne and ground geophysical data available from GTK were utilized. A total of about 500 thin sections were studied by petrographic microscope for their textures and modal compositions.

The petrographic classification of the Otanmäki suite igneous rocks was based on modal compositions obtained by point counting and the IUGS scheme. Garnet and biotite compositions for garnet-biotite thermometry and plagioclase compositions of the A-type rocks were determined at the Center of Microscopy and Nanotechnology, the University of Oulu, using a JEOL JXA-8200 electron microprobe (for EPMA results

see Electronic Appendix A3). The operating conditions were an acceleration voltage of 15 kV, a beam current of 10 nA, a spot size of 10 μm and peak and background counting times of 60 s and 30 s, respectively. The measured X-ray intensities were corrected by the ZAF method using chemical-known standard specimens. The quality of analysis was monitored by measuring natural garnet, biotite and plagioclase standards yielding a relative precision of $\pm 1.5\%$ and an accuracy of less than $\pm 1\%$ for the major oxides (SiO_2 , Al_2O_3 , TiO_2 , FeO , MnO , MgO , CaO , Na_2O , K_2O).

Whole-rock compositions were determined in three batches. The samples of the first two batches were analyzed at GTK and Labtium Oy using X-ray fluorescence (XRF), inductively coupled plasma mass spectrometry, optical emission spectrometry (ICP-MS/-OES) and LECO combustion analysis as the main methods (methods 175X, 308M, 308P, 811L, respectively; for more details, see Rasilainen et al., 2007). The sample batch analyzed at Labtium Oy included the USGS reference standard GSP-2 and one reference sample (117A-ATK-05) from the first analytical batch. An excellent correspondence of the results with the reference compositions was found (Electronic Appendix B). The third set of whole-rock samples was analyzed in the Bureau Veritas Minerals Canada Ltd by their method LF200, which involves lithium metaborate/tetraborate fusion, dissolution in ACS-grade nitric acid and analysis of major and trace elements by ICP-OES-MS. In addition, fluorine was analyzed separately by ICP-MS (method GC840) and total carbon and sulfur by LECO combustion analysis (method TC003). The rock samples were crushed and pulverized at the University of Oulu. For quality control, the same reference samples as in the batch analyzed at Labtium Oy were included. The correspondence between the analyses was excellent (Electronic Appendix B). In addition, we utilized five major and trace element analyses from the Rock Geochemical Database of Finland (Rasilainen et al., 2007) and four major element analyses from Marmo et al. (1966). Furthermore, we had access to unpublished major and trace element data obtained

at GTK in 1979–1985 using a Philips PW 1420/AHP spectrometer and fused (lithiumtetraborate) beads and those obtained at Rautaruukki Oy in 1977–1985 using a Philips PW1480 spectrometer and pressed powder pellets.

Multi-grain zircon U-Pb analyses were performed using a VG Sector 54 thermal ionization mass spectrometer and isotope dilution (ID-TIMS) at the isotope laboratory of the GTK. The method of the U-Pb TIMS analyses followed the procedures described in Huhma et al. (2018) and the analytical quality was on par with that in the given paper. Single grain U-Pb isotope analyses on zircon were made at the Finnish Isotope Geosciences Laboratory hosted by GTK in Espoo using a Nu Plasma HR multicollector ICP-MS instrument or a Nu Plasma AttoM single collector ICP-MS instrument connected to a Photon Machine Excite laser ablation system. The methods and related analytical quality control protocol are described in Huhma et al. (2018).

4. Geology of the Otanmäki suite

The main part of the Otanmäki suite A-type granites and intermediate igneous rocks are located in an E-W-trending, approximately 60-km-long and 1- to 10-km-wide belt covering an area of about 250 km^2 . As the sharply-defined boundaries of this belt appear to be faults involving significant displacements (for kilometers at least), we call this unit the Otanmäki-Kuluntalahti nappe or the main nappe (Fig. 2). This nappe is divided into three lithologically different parts, which are called the western, central and eastern segments (Fig. 2). The main nappe is bordered in the east by the Karelian formations of the Kainuu schist belt (Laajoki, 2005), and in north and the west, by Archean gneiss complexes (Vaasjoki et al., 2001; Hölttä et al., 2012b) (Fig. 2). The narrowest central part of the nappe is confined between Archean gneisses in the north and a narrow strip of Karelian supracrustal rocks in the south (Fig. 2). In addition, at closest some 0.5 km south of

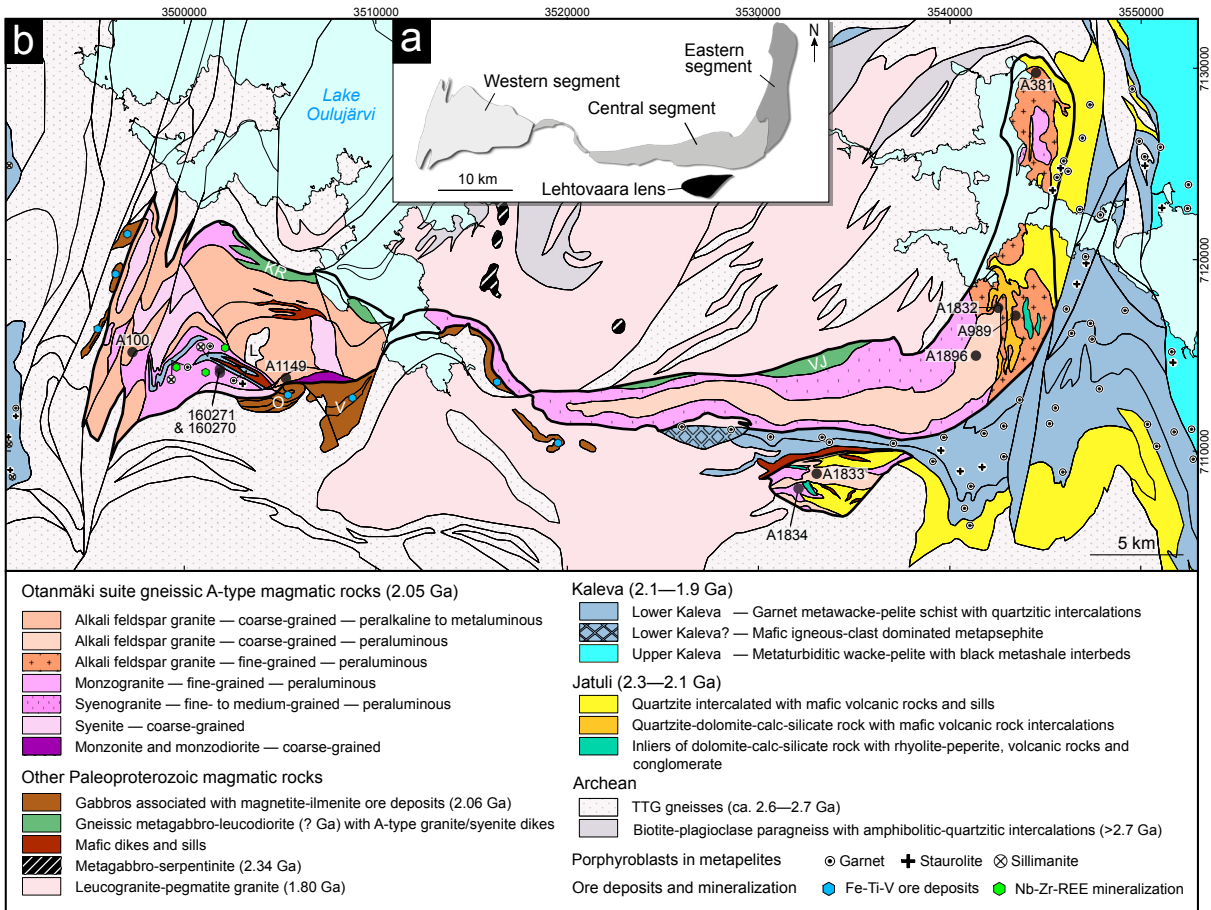


Figure 2. (a) Division of the Otanmäki-Kuluntalahti nappe into three segments and the Lehtovaara lens. (b) Geological map of the Otanmäki-Kuluntalahti nappe. O = Otanmäki gabbro, V = Vuorokas gabbro, L = Luodesuo Archean (?) enclave, KR = Kemiläistenräme mafic unit, VJ = Vuorijärvi mafic unit. Note that, for the sake of clarity, the ca. 1.80 Ga pegmatite granite dikes have been left unmarked within the Otanmäki-Kuluntalahti nappe and Lehtovaara lens and are shown as highly generalized masses outside them. Also shown are sample locations (black circles) for U-Pb zircon isotope analyses of this study. Coordinates in KJ-3/Finland Uniform Coordinate System.

the central segment of the main nappe, A-type rocks of the Otanmäki suite form a major intrusive phase in a 3x8-km-sized, fault-bound, lens-shaped body called the Lehtovaara lens (Fig. 2).

Both the Otanmäki-Kuluntalahti nappe and Lehtovaara lens are dominated by granitic rocks. In the QAP diagram, they plot in the fields of alkali feldspar (AF) granites, syenogranites and monzogranites (Fig. 3). The AF granites are further divided into three subtypes (Figs. 2 and 4–6): (1) coarse-grained, inequigranular AF granite with amphibole and/or clinopyroxene, forming the

bulk of the western segment, (2) coarse-grained, inequigranular AF granite with amphibole and biotite, occupying parts of the central segment and Lehtovaara lens, and (3) fine- to medium-grained, quartz±potassium feldspar-phyrlic biotite-bearing AF granite, forming a major component of the eastern segment. The syeno- and monzogranites contain varying amounts of biotite and amphibole, and are mostly fine-grained and equigranular rocks (Figs. 4–6). The syeno- and monzogranites are found in the Lehtovaara lens and the western and central segments, mostly bordering coarse-grained

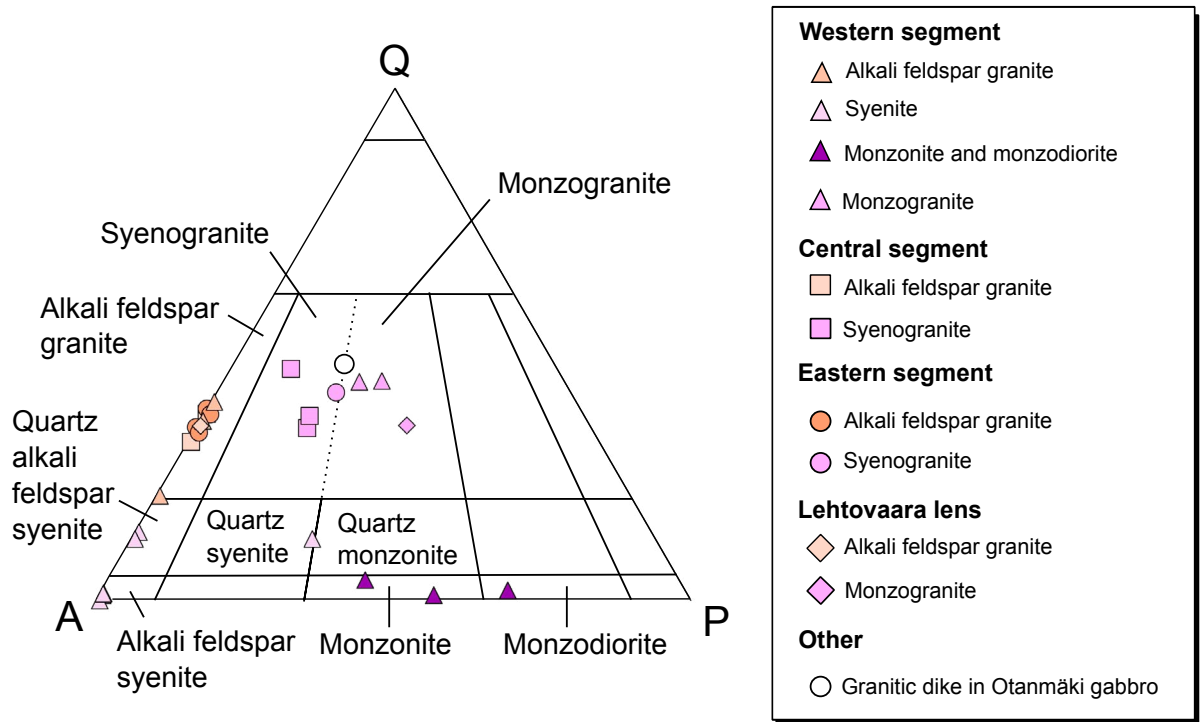


Figure 3. IUGS quartz-alkali feldspar-plagioclase (QAP) modal classification diagram (Streckeisen, 1976) for Otanmäki suite A-type rocks. Mineral abbreviations: Q = quartz, A = alkali feldspar (potassium feldspar, albite ($An < 5$)), and P = plagioclase ($An > 5$).

AF granites (Fig. 2). In addition, we have observed a few small bodies of medium-grained, amphibole-clinopyroxene syenogranite occurring in the eastern segment (Fig. 2).

Besides A-type igneous granitic rocks, the western segment of the main nappe also contains rocks with intermediate compositions (Fig. 2). Mostly these rocks are coarse- and even-grained syenites (Figs. 4–6) with their modal composition ranging from variably amphibole-, clinopyroxene- and/or biotite-bearing quartz AF syenite, AF syenite and quartz syenite (Fig. 3), which are all referred to as syenites in the subsequent chapters. Furthermore, there is a small body of coarse-grained, biotite-amphibole monzonite-monzodiorite (Figs. 3–5) at the southern margin of the western segment (Fig. 2). Hornblende-rich mafic enclaves (up to a meter across) also occur sporadically among the intermediate rocks and AF granites in the western segment (Fig. 4).

In outcrops, the Otanmäki suite A-type rocks are characterized by well-developed gneissic foliated and lineated fabrics (Figs. 4–5) indicative of a high degree of strain and mylonitization/cataclasis in their fabrics. Microstructures of the A-type rocks also reveal that they have been overprinted by a later recrystallization phase under static conditions (Fig. 6). Consequently, and considering the metamorphism in temperatures above 550 °C, it is difficult to judge how far (if not at all) the current minerals of the rocks represent their primary (igneous) mineralogy (for more detailed petrographic descriptions, see Electronic Appendix D).

In the regional geological pattern, one of the main expressions of the Svecofennian deformation is the sinistral S-fold shape of the central part of the Kainuu schist belt (Fig. 1), which is a result of N-S-trending sinistral wrench faulting and folding related to the orogen-parallel trans-compressional event in a late stage of the Svecofennian orogenesis, which

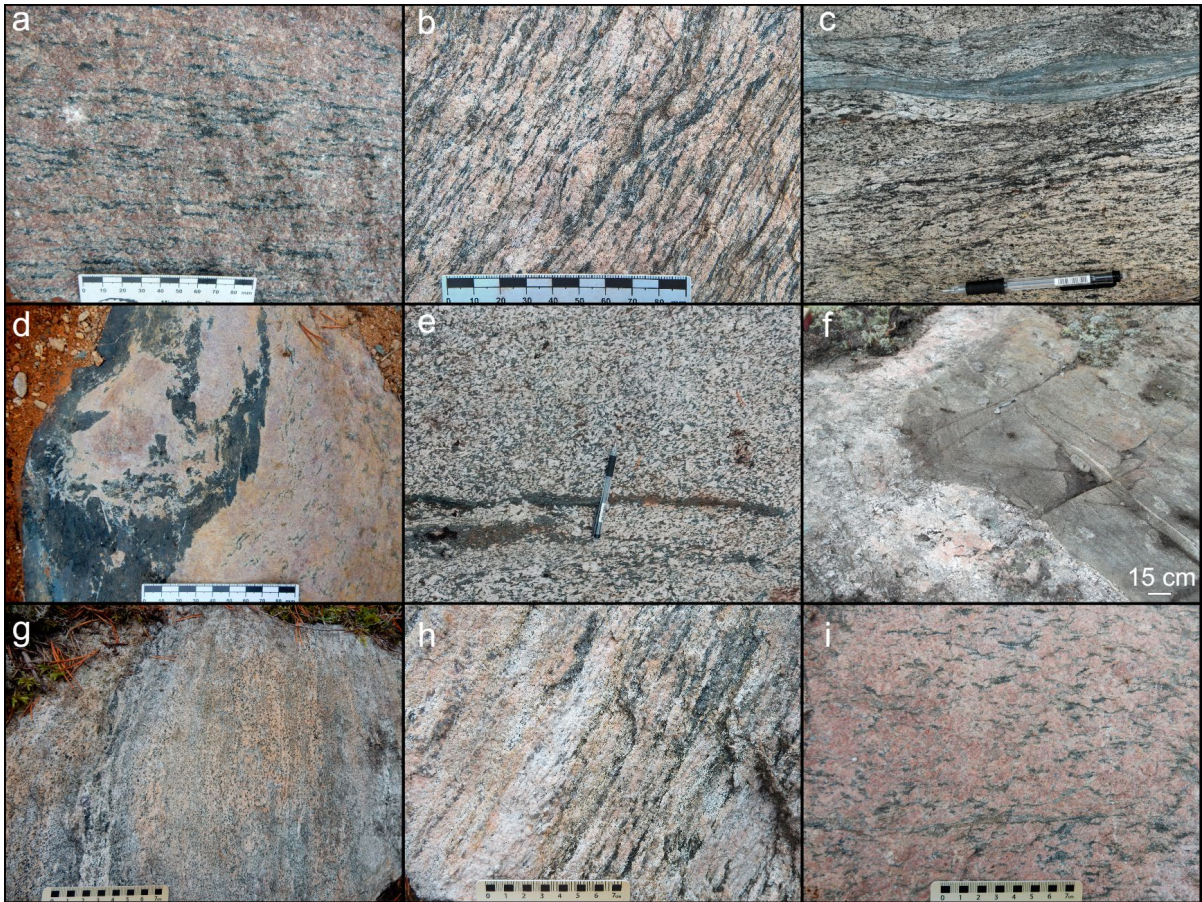


Figure 4. Outcrop photographs. (a) Coarse-grained alkali feldspar (AF) granite, western segment; (b) coarse-grained quartz AF syenite, western segment; (c) coarse-grained AF syenite, western segment; (d) hornblende-rich mafic enclave in AF syenite, western segment; (e) coarse-grained monzonite with mafic amphibole-rich bands, western segment; (f) fine-grained syenogranite (dark grey) cut by 1.80 Ga pegmatite granite dike (light grey), central segment; (g) fine-grained syenogranite, central segment; (h) lineated, coarse-grained AF granite, central segment; (i) AF granite with coarse potassium feldspar phenocrysts and fine-grained matrix, eastern segment. Pencil length in (c) and (e) 15 cm and scale bar in the other figures given in cms.

still shaped the rocks at the present erosional level in a considerable way. The structural features (foliation and lineation) in the Otanmäki suite nappes support their major shaping and anticlock-wise rotation in this final major structural event (see Electronic Appendix E). It can be speculated that before the rotation, the orientation of the longitudinal axis of the Otanmäki-Kuluntalahti nappe could have been SW-NE or even N-S. We also note that the gently ($\sim 10\text{--}30^\circ$) S- or SW-dipping foliations and lineations (Electronic Appendix E) in many parts of the Otanmäki-Kuluntalahti nappe record earlier

stages of the Svecofennian deformation, such as early thrusting.

As a consequence of the Svecofennian reworking and general poor exposure of contact zones, the original contact relationships between the fine-grained, subvolcanic-like granites and coarse-grained, obviously plutonic granites and intermediate rocks (e.g., contacts between AF granite and monzogranite blocks in the western segment, and those between syenogranite and AF granite in the central segment) are difficult to establish. In rare observed contact zones, it is still unclear whether

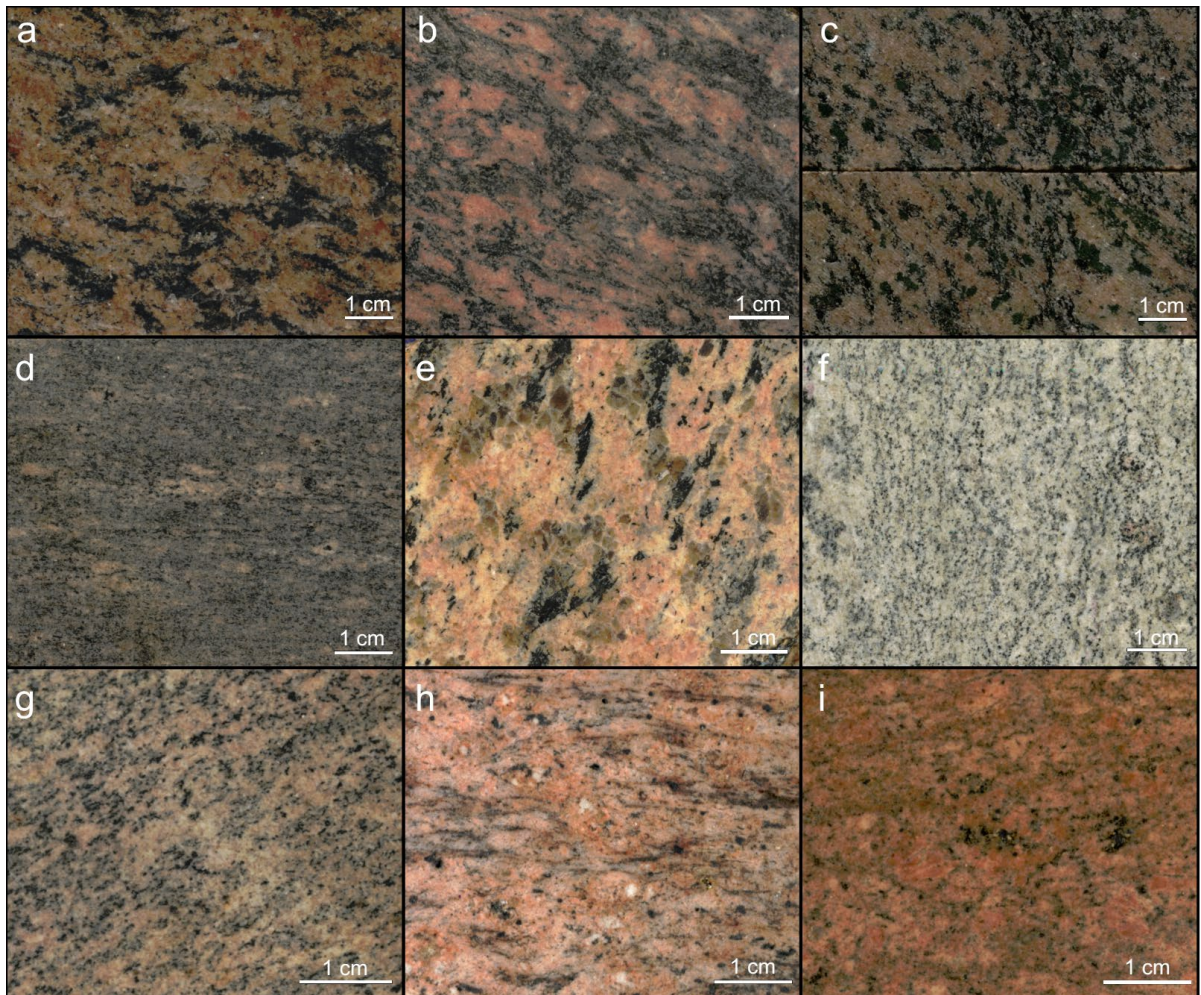


Figure 5. Photographs of polished slabs of typical Otanmäki suite granites and related intermediate rocks. (a) Alkali feldspar (AF) granite, (b) monzonite, (c) AF syenite, and (d) monzogranite from the western segment; (e) AF granite and (f-g) syenogranite from the central segment; (h-i) AF granite from the eastern segment.

the rock units had originally intrusive boundaries or whether they represent intrusive bodies emplaced originally at different crustal levels and are now stacked together by faults.

Another intriguing feature with the whole Otanmäki suite is the lack of observed intrusive contacts with gneisses of the surrounding Archean bedrock or lack of them as xenoliths. However, there is one potential occurrence of a country rock enclave in the western segment where a 2x3-km-sized block (Luodesuo enclave; Fig. 2) containing highly strained leucogranite and migmatitic

TTG-amphibolite gneisses is found, but without exposed contacts. These gneisses remain undated but have an appearance similar to those of typical Archean TTG-amphibolite-gneisses in the Karelia craton. Other potentially Archean gneissic units within the main nappe include tectonic slivers of metagabbroic-leucodioritic gneisses (at Kemiläistenrämme and Vuorijärvi; Fig. 2), which are intruded by yet undated A-type rocks (granite, syenite) in the form of small dikes or lenses. However, it is still unknown whether these mafic rocks represent the regional Archean bedrock, but as similar mafic rock

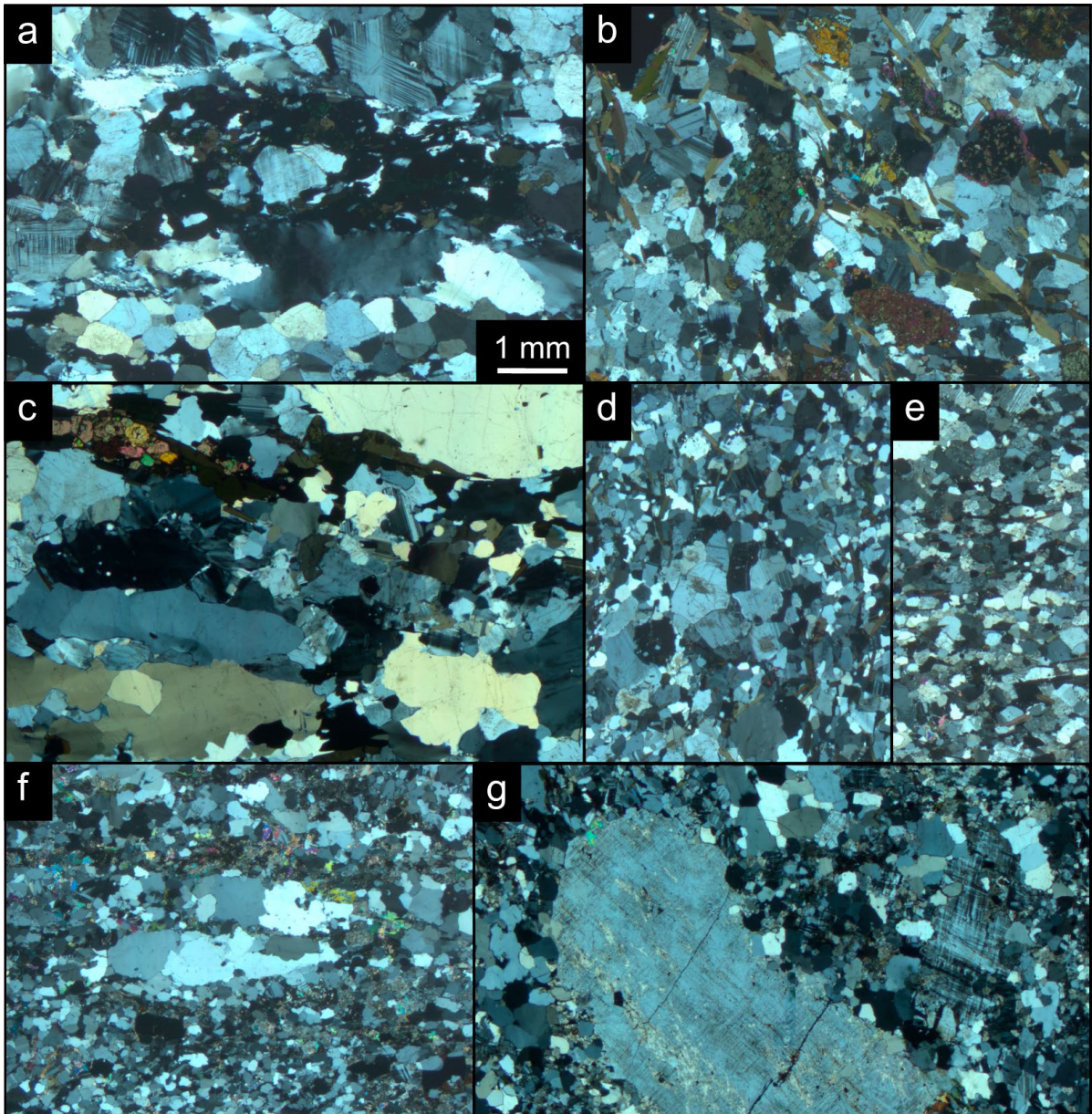


Figure 6. Photomicrographs (crossed-polars) of typical textures in Otanmäki suite A-type igneous rocks. (a) Alkali feldspar (AF) granite and (b) AF syenite, western segment; (c) AF granite and (d) syenogranite, central segment; (e) monzogranite, Lehtovaara lens; (f-g) quartz- and potassium feldspar-phyric AF granites, eastern segment. Scale in each figure is the same as in (a).

units have not been encountered elsewhere in the surrounding Archean complexes, it seems likely they are restricted in the Otanmäki-Kuluntalahti nappe.

Despite the scarcity of obvious Archean enclaves in the Otanmäki suite A-type rocks, in

several locations inside the main nappe and lens, fine-grained A-type granites (AF granite and syeno-monzogranite) enclose intrusive enclaves of supracrustal rocks a few m to several km in size, which bear similarities to Jatulian and Kalevian

cover and rift deposits (Fig. 2). Such supracrustal rocks include orthoquartzites with intercalations of dolomite and mafic volcanic rocks and sills in AF granite and monzogranite (eastern segment and Lehtovaara lens), metapsammite-pelite schist slivers in monzogranite (western segment), and amphibolite-calc-silicate rock enclaves in syenogranite (central segment). Furthermore, alongside with typical “Jatuli-type” sequences in the eastern segment and Lehtovaara lens, there are a number of small separate inliers containing volcanoclastic breccias and conglomerates (for more detailed descriptions, see Electronic Appendix D), which are uncommon in the Jatuli sequences in the Kainuu schist belt and have no obvious sources in the regional rock record (Laajoki, 2005).

It should be emphasized that in the study area, Otanmäki suite A-type rocks have so far been found only in the two nappes outlined above. The only known occurrence of potentially correlative A-type intrusive rocks outside the nappes are the A-type granite dikes found to crosscut the 2058 ± 15 Ma Otanmäki and Vuorokas gabbros (Fig. 2; Huhma et al., 2018), located just south of the western segment A-type rocks. However, the gabbros and A-type rocks of the western segment are in a vertical fault contact and show no evidence for intercalation.

5. U-Pb zircon geochronology

We report U-Pb isotope data for 10 A-type granite samples, of which 4 represent the western, 2 the central and 2 the eastern segment of the Otanmäki-Kuluntalahti nappe, and 2 samples come from the Lehtovaara lens. The locations of the analyzed granite samples are shown in Fig. 2 and their petrographic characteristics are described in Electronic Appendix C1. U-Pb data on zircon and titanite are listed in Electronic Appendix C1–4 and concordia plots of U-Pb zircon data are shown in Figs. 7 and 8.

Before we present the results of our U-Pb work, we must briefly consider the historical background

of dated samples as many of them were collected earlier by several investigators (GTK). Results of zircon U-Pb TIMS analyses done in the GTK between 1960s and 1990s from these old samples were also available to us. The very first reported zircon age of an Otanmäki suite granite was ca. 2.05 Ga, which was obtained by Marmo et al. (1966) for sample A100 (AF granite) taken from the western segment. This age was re-checked in the GTK in the 1980’s using the remaining zircon fractions of sample A100, yielding a younger age of 2.02 Ga (Hytönen & Hautala, 1985). A similar zircon age of 2.03 Ga (previously unpublished) was also produced in the 1970’s for zircon fractions from sample A381 (AF granite) taken by M. Asa and K. Meriläinen from the eastern segment. Even younger ages of ca. 1.96 Ga (previously unpublished) were produced in the 1990’s for zircons separated from two samples of AF granite (A1149 and A989) picked by M. Vaasjoki and M. Havola from the western and eastern segments. The 1.96 Ga ages are particularly interesting as they placed the Otanmäki suite temporally near the Jormua ophiolite complex (ca. 1.95 Ga), as was pointed out by Peltonen et al. (1996).

Because of the variability of the ages (2.05 to 1.96 Ga) produced previously, we reviewed the early TIMS results and noticed that many of the isotope compositions are discordant and display abnormal features, such as the heaviest zircon fractions being most discordant. Because of these observations, we decided to re-analyze the remaining zircon fractions from the old samples stored in the GTK. In order to better constrain the effects of metamorphism on the zircon ages, we utilized multigrain chemical abrasion (CA) TIMS method (Mattinson, 2005) and in-situ single grain analysis by LA-ICP-MS. We also collected new samples that represent AF granite (A1832, A1833, A1896) and monzogranite (A1834, 160270, 160271) from the western and central segments and Lehtovaara lens. From these samples, zircon and titanite were analyzed by the multigrain TIMS or by in-situ LA-MC-ICP-MS and LA-SC-ICP-MS methods. The results are

Table 1. Results of U-Pb zircon dating of Otanmäki suite granites.

Sample	Location	Northing	Easting	Rock type	Age/U-Pb TIMS produced previously	Age/U-Pb TIMS this study	Age/U-Pb LA-ICP-MS this study
Western segment							
A1149	Otanmäki, Kajaani	7113778	3505350	Peralkaline alkali feldspar granite	*1958 ± 29 Ma		2049 ± 10 Ma
A100	Honkamäki, Kajaani	7115100	3497400	Metaluminous alkali feldspar granite	*2020 ± 5 Ma		2041 ± 5 Ma
160271	Pieni-Katajakangas, Kajaani	7114244	3501926	Peraluminous monzogranite			2055 ± 8 Ma
160270	Pieni-Katajakangas, Kajaani	7114166	3501918	Peraluminous monzogranite			2060 ± 29 Ma
Central segment							
A1896	Kontinjärvi, Sotkamo	7114975	3541384	Peraluminous alkali feldspar granite		2050 ± 2 Ma	2053 ± 11 Ma
A1832	Kontinjoki, Sotkamo	7117515	3542542	Peraluminous alkali feldspar granite		2046 ± 3 Ma	
Eastern segment							
A989	Soidinvaara, Sotkamo	7117140	3543380	Peraluminous alkali feldspar granite	*1965 ± 13 Ma		
A381	Kuluntalahti, Kajaani	7129110?	3544400?	Peraluminous alkali feldspar granite	*2030 Ma		
Lehtovaara lens							
A1833	Käärmekalliot, Kajaani	7108790	3532953	Peraluminous alkali feldspar granite		2047 ± 3 Ma	
A1834	Niskalankalliot, Kajaani	7108099	3532151	Peraluminous monzogranite		2047 ± 5 Ma	

*Age reflects metamorphic effects on the primarily 2.05 Ga magmatic zircon, see text for details. Coordinates in KKKJ-3/Finland Uniform Coordinate System.

summarized in Table 1. The main reasons for the dated samples to be solely granites (AF granite and monzogranite) are historical as described above, but also the unfortunate timing of the discovery of the intermediate rocks in the very late stages of this study.

5.1 Western segment

A1149 (peralkaline AF granite). Results of four previous multigrain U-Pb TIMS analyses are available for this sample, obtained from an outcrop of coarse-grained AF granite 0.2 km north of the exposed fault contact to the Otanmäki gabbro intrusion. These data are discordant and define a chord with an upper intercept age of ca. 1.96 Ga (Fig. 7a). Recently, 36 grains from the remaining zircon fraction were analyzed by LA-MC-ICP-MS, including a total of 48 spot analyses, of which four were rejected due to a high amount of common lead. The obtained ages range from ca. 1.8 to 2.1 Ga and

define a bimodal distribution. Twenty one analyses from the older age group yield an age estimate of 2049 ± 10 Ma. These analyses were made on relatively clean, unaltered grain domains, whereas the data on altered-looking domains with a turbid appearance, fractures and micron-sized pores yield younger ages (Fig. 7a and Electronic Appendix C3). We therefore interpret 2049 ± 10 Ma as the probable magmatic age of the zircon and the younger data as results of metamorphic zircon re-equilibration. The new LA-MC-ICP-MS analyses also provide an explanation to the previous multigrain TIMS results as the latter obviously represent “average dates” of unaltered and altered zircon.

A100 (metaluminous AF granite). This sample was picked by Marmo et al. (1966) from a radioactively anomalous part in a large AF granite outcrop in the western part of the western segment. Zircon grains from sample A100 were already analyzed by O. Kouvo (GTK) in the 1960's, giving an age of ca. 2.05 Ga. This was the first age estimate

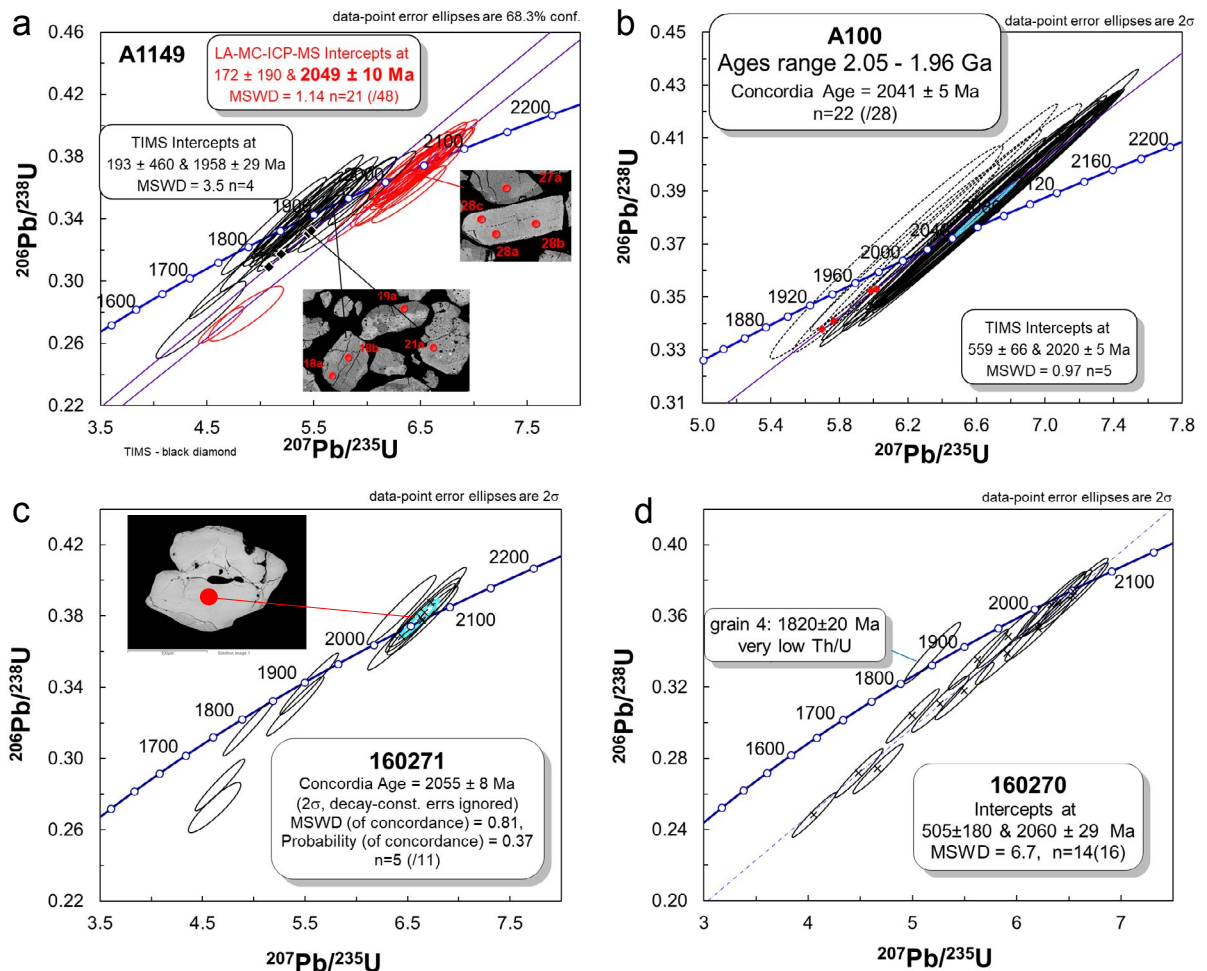


Figure 7. Concordia plots of U–Pb zircon data obtained for granite samples from the western segment. (a–b) Alkali feldspar (AF) granite samples A1149 and A100; (c–d) monzogranite samples 160271 and 160270. LA-MC-ICP-MS analyses are shown as error ellipsoids. In (a) and (b), the ID-TIMS data are shown as dots because 2-sigma error ellipses would be smaller than the dots. For the sake of clarity, error ellipses in (a) are shown at 1-sigma.

obtained for a granitic rock from the Otanmäki suite and published by Marmo et al. (1966). However, the age was later checked by O. Kouvo using five zircon fractions, which together gave a slightly younger age estimate of ca. 2.02 Ga (published by Hytönen & Hautala, 1985). In this study, a fraction of the remaining zircon grains from sample A100 was analyzed by LA-MC-ICP-MS, resulting in 28 concordant compositions (within analytical error) defining ages between 2.05 and 1.96 Ga (Fig. 7b). As was discussed above, the younger dates are likely due to metamorphic effects. Excluding

six such analyses, the data yield a $^{207}\text{Pb}/^{206}\text{Pb}$ age of 2041 ± 5 Ma, which is considered a minimum age of the dated granite.

160271 and 160270 (peraluminous monzogranite). These samples were collected from two closely located outcrops of fine-grained monzogranite located in the middle part of the western segment. They were used for zircon dating by LA-MC-ICP-MS directly from thin sections. A total of 11 spots from 9 zircon crystals were analyzed from sample 160271 (Fig. 7c). Five spots ($n = 5/11$) show consistent results defining a concordia age of

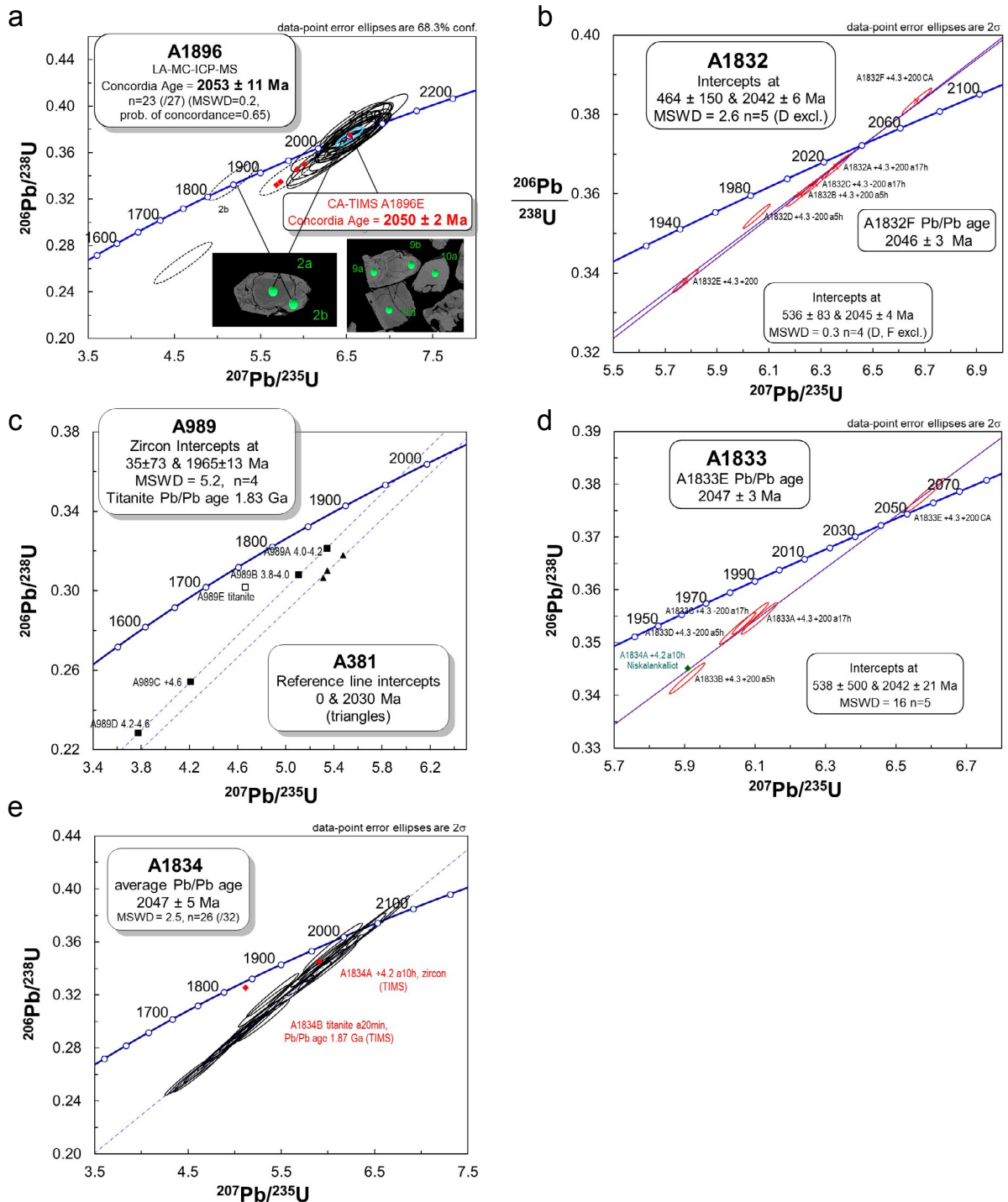


Figure 8. Concordia plots of U-Pb zircon data obtained for granite samples. (a) and (b) Alkali feldspar (AF) granite samples A1896 and A1832, respectively, from the central segment; (c) AF granite samples A989 and A381 from the eastern segment; and (d) monzogranite sample A1834 and (e) AF granite sample A1833 from the Lehtovaara lens. LA-MC-ICP-MS data are shown as error ellipsoids. In (b) and (d) TIMS data are shown as error ellipsoids, but in (a), (c) and (e), TIMS data are shown by dots because 2-sigma error ellipses would be smaller than the dots. For the sake of clarity, in (a), error ellipses are at 1-sigma.

2055 ± 8 Ma, which is considered the best estimate for the age of magmatic crystallization. Other data show younger Pb/Pb ages and mostly low Th/U ratios suggesting metamorphic effects. Sixteen spots in 12 zircon grains were measured from sample 160270. Excluding two analyses, the U-Pb data plot roughly on a chord, giving an upper intercept age of ca. 2.06 Ga (Fig. 7d). One of the excluded zircon grains has very low Th/U and is concordant at 1.82 Ga and another is Archean in age, attesting to the presence of xenocrystic material (Fig. 7d).

5.2 Central segment

A1896 (peraluminous AF granite). Sample A1896 was taken from a coarse-grained AF granite located close to the eastern margin of the central segment. Mineral separation yielded abundant mostly euhedral, slightly turbid zircon and titanite. Four conventional ID-TIMS, one CA-TIMS and 27 LA-MC-ICP-MS analyses were performed on the zircon separate. The ID-TIMS analyses gave compositions plotting on a discordia line with intercepts at 2025 ± 5 and 121 ± 120 Ma (MSWD = 0.1, Fig. 8a). The unusually low upper intercept is practically defined by two points representing +200 and -200 (mesh) zircon size fractions (Fig. 8a). It is conceivable that the discordia pattern is variable in different size fractions, reflecting 1.8–1.9 Ga metamorphic effects. Additional evidence for such effects in this sample is provided by titanite, which yielded a ²⁰⁷Pb/²⁰⁶Pb age of ca. 1.83 Ga (see Electronic Appendix C2). A similar age for titanite was obtained from a sample of AF granite (A989) picked approximately 3 km northeast of the location of sample A1896 (see below). Previous titanite U-Pb dating from many other rocks in the Svecofennia-Karelia boundary zone has produced similar titanite ages (1.80–1.87 Ga) (Isotope data of Finnish bedrock; <https://hakku.gtk.fi/en>). The analysis using chemical abrasion (CA-TIMS) yielded an extremely low common lead abundance (²⁰⁶Pb/²⁰⁴Pb >40 000) and a concordant age at 2050 ± 2 Ma. This age is considered the crystallization time of magmatic zircon and the emplacement

age of the AF granites in the central segment. The majority of the 27 LA-MC-ICP-MS analyses on 23 grains from sample A1896 produced concordant results, although with large error margins due to calibration issues. Nevertheless, the reproducibility of the LA-MC-ICP-MS analyses was good and the analyses of standard A1772 implied that systematic error cannot be significant. Excluding four analyses, the data yield a concordant age estimate of 2053 ± 11 Ma (Fig. 8a). One analysis from the rim of a zircon crystal gives a younger age of ca. 1.83 Ga (Fig. 8a), which is similar to the age obtained for titanite.

A1832 (peraluminous AF granite). Sample A1832 was taken from an outcrop of medium- to coarse-grained AF granite located 3 km north of the location of sample A1896. Mineral separation yielded abundant subhedral, fairly short zircon grains ranging from turbid to fairly translucent in appearance. Most grains are in the -200 mesh (<70 µm) fraction. The U-Pb analyses by ID-TIMS are technically of normal good quality and show that the common lead content of the zircon grains is low. However, one of the six isotope compositions is off the chord defined by the rest of the data, and one of the CA-TIMS compositions plots slightly above the concordia curve (Fig. 8b). Excluding these two analyses, the data yield intercepts at 2045 ± 4 and 536 ± 83 Ma (MSWD = 0.3). Some unconstrained U/Pb fractionation could be involved in the CA-TIMS analysis, but it is likely that the ²⁰⁷Pb/²⁰⁶Pb age of 2046 ± 3 Ma most closely dates the magmatic crystallization of the sampled AF granite.

5.3 Eastern segment

A989 (peraluminous AF granite). Sample A989 (fine-grained and phyric AF granite) was taken from the southern part of the eastern segment about 0.8 km east of sample A1832 discussed above. Four zircon density fractions show discordant compositions defining a chord with an upper intercept U-Pb age of 1965 ± 13 Ma (Fig. 8c). The data reveal a rather unusual relationship, since the analytical results for the heavy fractions are more

discordant than those for the light fractions. The unexpectedly young upper intercept age is similar to that obtained by multigrain TIMS analysis for sample A1149, as discussed above. Consequently, it is very likely that the TIMS age of sample A989 also represents metamorphic effects on a ca. 2.05 Ga magmatic zircon. A titanite fraction yielded a discordant composition providing a $^{207}\text{Pb}/^{206}\text{Pb}$ age of ca. 1.83 Ga.

A381 (peraluminous AF granite). Sample A381 is from a somewhat uncertain locality within the northern part of the eastern segment. The first U-Pb analyses for zircon grains from this sample were performed by O. Kouvo in 1971, using the borax-fusion method for dissolution and an in-house-built TIMS mass spectrometer at the GTK for the isotope analysis. These early and two subsequent multi-grain TIMS analyses produced discordant $^{207}\text{Pb}/^{206}\text{Pb}$ ages of ca. 2.03 Ga (Fig. 8c). We are inclined to think that this result reflects metamorphic effects on the primarily 2.05 Ga magmatic zircon.

5.4 Lehtovaara lens

A1833 (peraluminous AF granite). Sample A1833 was picked from the Lehtovaara lens and represents a coarse-grained AF granite, which is petrographically nearly identical to sample A1832. Mineral separation yielded abundant zircon grains, which are fairly similar to those obtained from sample A1832. The analytical results of four conventional U-Pb analyses are slightly discordant, have limited Pb/U and yield $^{207}\text{Pb}/^{206}\text{Pb}$ ages of ca. 2.02–2.03 Ga. Instead, the CA-TIMS analysis gives practically concordant data, with a $^{207}\text{Pb}/^{206}\text{Pb}$ age of 2047 ± 3 Ma, which is considered to be the age of magmatic zircon (Fig. 8d).

A1834 (peraluminous monzogranite). Another sample from the Lehtovaara lens, A1834, represents monzogranite similar to samples 160271 and 160270 from the western segment. Mineral separation yielded subhedral, translucent zircon grains and abundant titanite. A total of 32 spot analyses on 27 zircon crystals were made by

LA-SC-ICP-MS. The obtained compositions are variably discordant, plotting roughly on a chord which suggests an upper intercept age of ca. 2.05 Ga. However, there is some scatter potentially related to metamorphic effects as discussed above. Excluding few analyses with elevated common lead, an average $^{207}\text{Pb}/^{206}\text{Pb}$ age of 2047 ± 5 Ma can be calculated (Fig. 8d). The composition measured by U-Pb TIMS for one multigrain zircon fraction is discordant, yet consistent with the ICP-MS data. Also one U-Pb TIMS composition obtained for titanite is slightly discordant, providing a $^{207}\text{Pb}/^{206}\text{Pb}$ age of ca. 1.87 Ga (Fig. 8d).

6. Geochemistry

This study employs a total of 182 whole-rock chemical analyses of the Otanmäki suite, representing the whole range of A-type igneous rocks identified in this work. In addition, one analysis is from a foliated A-type granite dike cross-cutting the 2.06 Ga Otanmäki gabbro intrusion. Representative compositions of Otanmäki suite igneous rocks are presented in Table 2 (for a complete list of analyses, see Electronic Appendix B).

6.1 Major and trace elements

The Otanmäki suite igneous rocks show a wide range in SiO_2 contents covering a spectrum from monzodioritic-monzonitic (47–59 wt.%) to syenitic (52–65 wt.%) and granitic (65–78 wt.%) rocks. A common feature for the main rock types is a high content of total alkalis, 6–12 wt.% in granites, 9–13 wt.% in the syenites, and 6–10 wt.% in monzonites and monzodiorites. They are all ferroan, except for a few AF granite samples from the eastern segment which are magnesian likely due to synemplacement interaction with dolomites at AF granite-dolomite contacts (Fig. 9a).

The petrographic characteristics and chemical compositions of the granitic rocks located within the Otanmäki-Kuluntalahti nappe and Lehtovaara lens suggest that there are four different granite

Table 2. Representative whole-rock compositions of Otanmäki suite granites and intermediate rocks.

Location	WS	LL	CS	CS	ES	WS	WS	CS	CS	CS	
Sample	212A- ATK-06	391-ATK- 05/A1834	212- ATK-05	KAKA- 2016-93	KAKA- 2016- 266	117A- ATK-06	KA-R8- 53.27- 53.57m	398i- ATK- 06/1896	ATK- 2016- 660.1	216i- ATK- 05/1832	
Rock type	Monzogr.	Monzogr.	Syenogr.	Syenogr.	Syenogr.	AFgr.	AFgr.	AFgr.	AFgr.	AFgr.	
Northing	7114166	7108008	7112254	7111711	7126705	7115730	7116408	7114975	7112743	7117515	
Easting	3501918	3532538	3540837	3519579	3544774	3497360	3501010	3541384	3536551	3542542	
SiO ₂	71.30	69.30	65.70	70.35	66.40	73.39	68.34	72.50	69.80	75.00	wt.%
TiO ₂	0.88	0.87	1.24	0.82	1.03	0.27	0.32	0.36	0.47	0.27	wt.%
Al ₂ O ₃	13.00	13.40	13.60	12.75	13.39	11.71	11.37	13.30	13.68	12.30	wt.%
FeO _{tot}	2.99	4.30	5.71	3.72	6.01	3.43	7.35	2.82	4.18	2.31	wt.%
MnO	0.08	0.09	0.07	0.09	0.08	0.10	0.13	0.06	0.12	0.02	wt.%
MgO	0.35	0.78	0.92	0.49	1.44	0.13	0.55	0.26	0.29	0.18	wt.%
CaO	3.25	1.91	3.29	5.67	2.75	0.83	1.80	1.09	1.25	0.78	wt.%
Na ₂ O	2.53	3.44	4.53	1.05	3.83	4.43	5.23	4.00	3.91	3.65	wt.%
K ₂ O	4.37	4.70	3.61	4.80	3.42	4.64	3.89	4.80	5.26	4.73	wt.%
P ₂ O ₅	0.20	0.22	0.25	0.22	0.27	0.03	0.02	0.05	0.06	0.03	wt.%
F	n.d.	n.d.	n.d.	n.d.	0.12	0.33	n.d.	n.d.	0.07	n.d.	wt.%
C	0.33	0.08	0.02	<0.05	<0.02	<0.02	0.07	0.02	<0.02	0.10	wt.%
S	<0.01	n.d.	n.d.	n.d.	0.11	<0.02	<0.01	n.d.	0.00	n.d.	wt.%
Cl	0.01	0.02	0.01	0.00	n.d.	0.00	0.00	0.02	n.d.	0.02	wt.%
Total	99.28	99.12	98.93	99.96	98.85	99.28	99.07	99.27	99.09	99.40	wt.%
LOI	n.d.	n.d.	n.d.	n.d.	0.40	0.40	n.d.	n.d.	0.20	n.d.	wt.%
Co	5.0	7.1	8.8	4.1	n.d.	0.5	0.7	1.5	n.d.	1.0	ppm
V	66	34	67	35	56	<8	<5	<0.5	<8	1.0	ppm
Sc	8.6	9.6	10	8.6	9.0	<1	5.2	3.9	4.0	2.7	ppm
Nb	45	48	43	26	34	146	346	69	54	64	ppm
Ta	2.9	3.0	2.6	1.8	2.1	8.2	15	4.2	3.0	4.4	ppm
Zr	366	399	308	312	207	957	1505	512	519	542	ppm
Hf	8.8	11	7.6	6.5	5.2	23	36	13	12	15	ppm
Ba	1050	1080	987	474	962	221	39	1000	1131	457	ppm
Sr	195	203	180	90	316	21	26	88	100	35	ppm
Rb	135	147	110	156	79	164	384	156	117	172	ppm
Th	16	18	15	12	10	27	69	18	15	19	ppm
U	4.2	4.9	4.4	4.0	4.0	7.5	13	5.3	3.3	3.5	ppm
Ga	26	28	27	25	21	26	40	31	23	32	ppm
Mo	<10	<10	<10	<10	n.d.	n.d.	<10	<10	n.d.	<10	ppm
Pb	31	25	24	<30	n.d.	n.d.	<30	15	n.d.	30	ppm
Sn	<20	<20	<100	<30	2.0	n.d.	45	<100	3.0	<20	ppm
Y	39	39	35	31	27	84	176	47	34	46	ppm
La	61	64	59	57	52	125	255	91	71	100	ppm
Ce	131	136	117	120	104	237	520	191	140	208	ppm
Pr	15	16	14	14	13	28	59	22	16	23	ppm
Nd	60	64	56	55	52	100	207	85	63	88	ppm

Table 2. (cont.)

Location	WS	LL	CS	CS	ES	WS	WS	CS	CS	CS	
Sample	212A- ATK-06	391-ATK- 05/ A1834	212- ATK-05	KAKA- 2016-93	KAKA- 2016- 266	117A- ATK-06	KA-R8- 53.27- 53.57m	398i- ATK- 06/A1896	ATK- 2016- 660.1	216i- ATK- 05/A1832	
Rock type	Monzog.	Monzog.	Syenogr.	Syenogr.	Syenogr.	AF gr.	AF gr.	AF gr.	AF gr.	AF gr.	
Northing	7114166	7108008	7112254	7111711	7126705	7115730	7116408	7114975	7112743	7117515	
Easting	3501918	3532538	3540837	3519579	3544774	3497360	3501010	3541384	3536551	3542542	
Sm	11	11	10	10	9.3	19	40	15	11	14	ppm
Eu	2.6	2.5	2.3	2.1	2.7	2.3	4.8	2.4	2.7	1.4	ppm
Gd	11	11	9.1	8.1	8.1	17	38	13	9.1	13	ppm
Tb	1.5	1.5	1.3	1.1	1.1	2.8	6.1	1.8	1.3	1.8	ppm
Dy	7.2	7.6	6.5	6.2	5.9	17	38	9.0	7.2	8.5	ppm
Ho	1.4	1.5	1.2	1.2	1.1	3.4	7.5	1.6	1.4	1.6	ppm
Er	3.6	3.9	3.3	3.2	2.9	9.5	20	4.5	3.8	4.4	ppm
Tm	0.5	0.6	0.4	0.4	0.4	1.3	2.6	0.6	0.5	0.6	ppm
Yb	3.2	3.5	3.0	2.6	2.4	7.8	16	4.1	3.2	3.8	ppm
Lu	0.4	0.5	0.5	0.4	0.4	1.1	2.4	0.6	0.5	0.6	ppm

Location	LL	ES	ES	WS	WS	WS	WS	WS	WS	
Sample	383i- ATK- 05/ A1833	5-OTA- 92	206- ATK-05	KAKA- 2017-5	VJ-R1- 88.20- 88.70m	MHR- 150694	KAKA- 2016-20	KAKA- 2016- 183	KAKA- 2017-3	
Rock type	AF gr.	AF gr.	AF gr.	AF sye.	AF sye.	Qtz. AF sye.	Qtz. sye.	Monz.	Monzodior.	
Northing	7108790	7117130	7127820	7117426	7115404	7118630	7113030	7114046	7113942	
Easting	3532953	3543390	3545059	3496581	3507425	3504110	3504680	3506975	3507168	
SiO ₂	74.90	72.02	72.50	63.58	60.21	62.30	55.42	55.56	47.78	wt.%
TiO ₂	0.28	0.44	0.48	0.58	0.75	0.84	0.21	1.26	2.61	wt.%
Al ₂ O ₃	12.20	12.74	13.20	14.72	16.70	15.50	21.50	16.83	16.12	wt.%
FeO _{tot}	2.30	3.95	3.20	6.84	7.13	6.67	5.87	8.98	12.28	wt.%
MnO	0.05	0.09	0.03	0.16	0.22	0.21	0.16	0.25	0.24	wt.%
MgO	0.23	0.38	0.48	0.06	0.58	0.40	0.20	1.26	2.26	wt.%
CaO	0.68	0.51	0.73	1.31	2.40	2.15	2.26	4.32	8.07	wt.%
Na ₂ O	3.69	2.95	4.24	6.46	6.19	5.75	7.88	5.80	4.70	wt.%
K ₂ O	4.79	5.94	4.35	5.17	4.83	4.69	5.54	3.47	1.74	wt.%
P ₂ O ₅	0.03	0.07	0.08	0.03	0.26	0.21	0.09	0.57	1.41	wt.%
F	n.d.	n.d.	n.d.	0.27	n.d.	0.04	n.d.	n.d.	0.11	wt.%
C	0.08	0.10	0.02	<0.02	0.06	0.06	<0.05	<0.05	<0.02	wt.%
S	n.d.	n.d.	n.d.	<0.02	0.04	0.02	0.00	0.02	0.07	wt.%
Cl	0.02	0.02	0.01	n.d.	0.00	0.03	0.00	0.01	n.d.	wt.%
Total	99.25	99.20	99.32	99.18	99.38	98.87	99.13	98.33	97.39	wt.%
LOI	n.d.	0.86	n.d.	0.20	n.d.	n.d.	n.d.	n.d.	0.90	wt.%
Co	1.0	n.d.	2.2	n.d.	3.6	2.4	2.9	8.4	n.d.	ppm
V	0.9	27.0	5.6	<8	<5	1.2	<5	<5	33	ppm
Sc	3.4	1.0	4.9	<1	4.7	4.6	1.4	7.1	13	ppm

Table 2. (cont.)

Location	LL	ES	ES	WS	WS	WS	WS	WS	WS	
Sample	383i- ATK- 05/A1833	5-OTA -92	206- ATK-05	KAKA- 2017-5	VJ-R1- 88.20- 88.70m	MHR- 150694	KAKA- 2016-20	KAKA- 2016-183	KAKA- 2017-3	
Rock type	AF gr.	AF gr.	AF gr.	AF sye.	AF sye.	Qtz. AF sye.	Qtz. sye.	Monz.	Monzodior.	
Northing	7108790	7117130	7127820	7117426	7115404	7118630	7113030	7114046	7113942	
Easting	3532953	3543390	3545059	3496581	3507425	3504110	3504680	3506975	3507168	
Nb	77	43	44	49	55	64	50	44	9.0	ppm
Ta	5.4	4.6	n.d	2.2	2.5	2.6	2.9	2.2	0.5	ppm
Zr	518	350	320	194	102	244	160	89	68	ppm
Hf	15	20	8.7	4.8	4.1	5.25	6.16	3.5	1.6	ppm
Ba	627	1300	914	98	870	2410	564	5956	2832	ppm
Sr	40	68	115	11	96	239	163	714	823	ppm
Rb	160	245	94	111	99	76	97	55	21	ppm
Th	21	21	19	7.6	4.7	6.0	6.5	5.0	1.3	ppm
U	4.3	5.0	4.4	1.3	0.5	1.0	0.8	0.5	0.3	ppm
Ga	29	25	29	36	27	34	28	16	18	ppm
Mo	<10	0.0	<10	n.d	<10	0.0	<10	<10	n.d	ppm
Pb	38	24	<30	n.d	<30	22	<30	<30	n.d	ppm
Sn	<20	2.0	<20	2.0	<30	n.d	<30	<30	<1	ppm
Y	41	25	32	25	17	28	22	21	15	ppm
La	64	72	54	70	32	44	35	41	18	ppm
Ce	140	145	118	131	68	96	73	83	44	ppm
Pr	16	17	13	15	8.5	12	8.8	10	6.6	ppm
Nd	61	64	53	53	34	48	34	42	33	ppm
Sm	11	18	9.4	8.5	5.9	8.4	6.0	7.5	6.7	ppm
Eu	1.4	4.6	2.0	1.2	2.2	3.6	1.7	5.5	4.6	ppm
Gd	11	16	8.8	6.8	5.0	7.8	5.4	6.5	6.3	ppm
Tb	1.5	2.2	1.2	0.9	0.7	1.1	0.8	0.8	0.8	ppm
Dy	8.0	8.0	6.0	5.2	3.7	5.1	4.6	4.5	3.7	ppm
Ho	1.5	1.3	1.1	1.0	0.7	1.0	0.9	0.8	0.6	ppm
Er	4.1	4.4	3.1	2.8	1.8	2.6	2.5	2.1	1.4	ppm
Tm	0.6	0.6	0.4	0.4	0.3	0.3	0.4	0.3	0.2	ppm
Yb	3.8	3.6	2.8	3.1	1.8	2.4	2.4	1.6	1.1	ppm
Lu	0.6	0.6	0.5	0.6	0.3	0.3	0.4	0.3	0.2	ppm

WS = Western segment; CS = Central segment; ES = Eastern segment; LL = Lehtovaara lens; Monzogr., monzogranite; Syenogr., syenogranite; AF gr., alkali feldspar granite; AF .sye., alkali feldspar syenite; Qtz. AF sye., quartz alkali feldspar syenite; Qtz.sye., quartz syenite; Monz., monzonite; Monzodior., monzodiorite; n.d = not determined; LOI = loss of ignition. Coordinates in KJ-3/Finland Uniform Coordinate System.

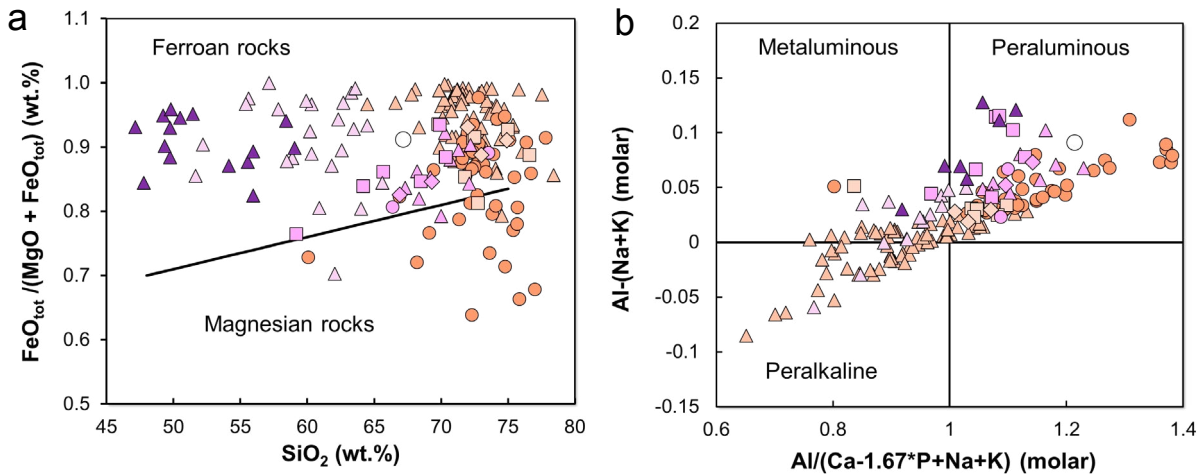


Figure 9. Major element classification diagrams for Otanmäki suite granites and related intermediate rocks. (a) $\text{FeO}_{\text{tot}}/(\text{MgO} + \text{FeO}_{\text{tot}})$ vs. SiO_2 diagram (Frost & Frost, 2008) showing fields for ferroan and magnesian igneous rocks. (b) Alkalinity index (molar $\text{Al}-(\text{Na} + \text{K})$) vs. alumina saturation index ($\text{ASI} = \text{Al}/(\text{Ca} - 1.67 * \text{P} + \text{Na} + \text{K})$ in molar units) diagram, which distinguishes peralkaline, metaluminous, and peraluminous igneous rocks (Frost & Frost, 2008). Symbols as in Fig. 3.

phases: 1) coarse-grained, peralkaline-metaluminous AF granites, 2) coarse-grained, peraluminous AF granites, 3) fine-grained, peraluminous AF granites, and 4) fine-grained, peraluminous syeno-monzogranites (Figs. 9–13). The peralkaline-metaluminous AF granites are strongly depleted in P, Ti, Sr, Eu and Ba relative to REEs (Fig. 12), which is indicative of feldspar, apatite and ilmenite/magnetite fractionation. These granites also have the highest contents of REEs, Y, Zr and Nb in the suite and are variably enriched in Th-U, Nb-Ta and Zr-Hf relative to REEs (except Eu), unlike the other granite types (Figs. 11 and 12). The peraluminous granite types (coarse- and fine-grained AF granite and syeno-monzogranites) are in general less depleted in Ba, Sr, Eu, Ti and P (relative to REEs, except Eu) compared to the peralkaline-metaluminous AF granites (Fig. 12), indicating that they are less evolved. A common feature in all peraluminous granites is their depletion in Nb-Ta and enrichment in Th-U relative to REEs (except Eu), which could be a consequence of crustal contamination (Fig. 12). The syeno-monzogranites appear to be less evolved compared to the peraluminous AF granites based on their higher FeO_{tot} , TiO_2 , P_2O_5 , Co and Sc contents and Eu/

Eu* ratio, supporting the view that they represent a separate granite phase (Figs. 10 and 11). It is also important to mention that the granite dike cutting the Otanmäki gabbro has a similar composition to that of the syeno-monzogranites in the Otanmäki suite (Figs. 9–13), thus demonstrating that the dike cannot be an apophyse from the western segment peralkaline-metaluminous AF granites situated north of the Otanmäki gabbro.

The intermediate rock samples range from peralkaline to peraluminous, but most of them are metaluminous or marginally peraluminous (Fig. 9b). In comparison to the granites, the intermediate rocks show mostly higher contents of Na_2O , TiO_2 , FeO_{tot} , MnO, CaO, and P_2O_5 and trace elements considered compatible in feldspars and mafic silicates (e.g., Eu, Co, Sc, Sr, and Ba) and have lower contents of incompatible elements (e.g., Zr, REE, Y, Rb, Th and U) (Figs. 10 and 11). In terms trace elements, the syenites are mostly intermediate between granites and monzonite-monzodiorite with partly overlapping compositions (Fig. 11). They show a moderate depletion in P and Ti and an enrichment in K, but a minor depletion in Zr-Hf, Th-U and Nb-Ta relative to REEs (except Eu) (Fig. 12). Based on their Ba, Eu and

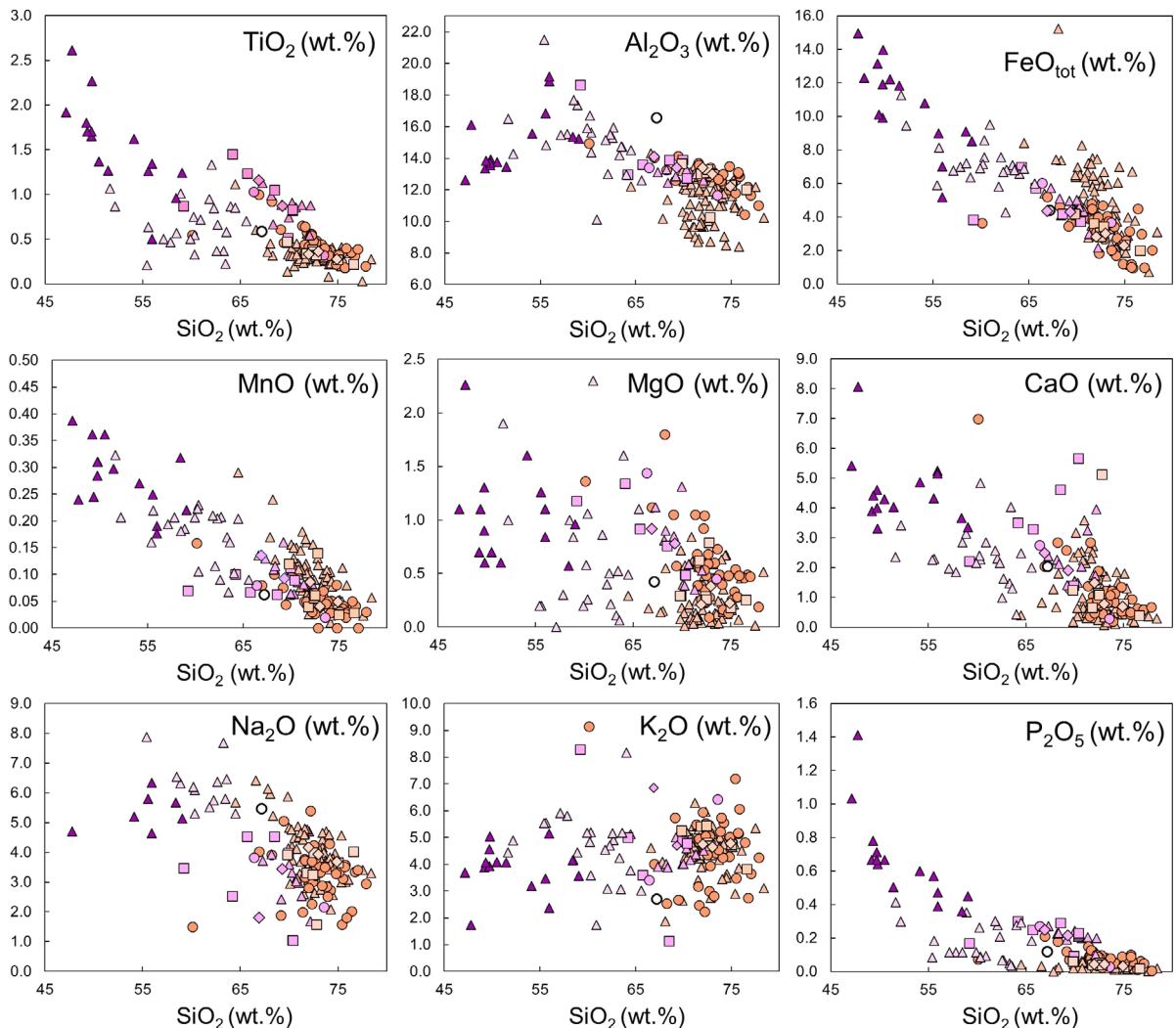


Figure 10. Harker diagrams for major elements in Otanmäki suite granites and intermediate rocks. Symbols as in Fig. 3.

Sr contents, the syenites can be subdivided into Ba-Sr-Eu-depleted and -enriched types, indicating that the syenites may have evolved by feldspar fractionation from a common parental magma (Fig. 12). The monzonitic and monzodioritic rocks have very similar trace element compositions with enrichments in Ba, Eu, Sr and K (suggesting feldspar accumulation) relative to REEs (Fig. 12). In addition, unlike the granites and syenites, they lack depletion in P and Ti and show depletion in Th-U and Nb-Ta relative to REEs (except Eu) (Fig. 12).

The granites and intermediate rocks all display fairly consistently flat OIB-normalized REE

patterns (excluding variable Eu anomalies discussed above) (Fig. 13), with no obvious secondary effects such as LREE depletion, not even in the samples from the locally REE-mineralized western segment (Fig. 2; Kärenlampi et al., 2017). This indicates that suitable REE-mobilizing ligands were largely absent in fluids that passed through the A-type rock bodies during metamorphism. In addition, compared to non-metamorphosed A-type suites, the Otanmäki suite A-type rock samples have very similar major and trace element patterns and concentration levels (see chapter 7.1). Therefore, it seems justified that despite the strong Svecofennian tectonothermal

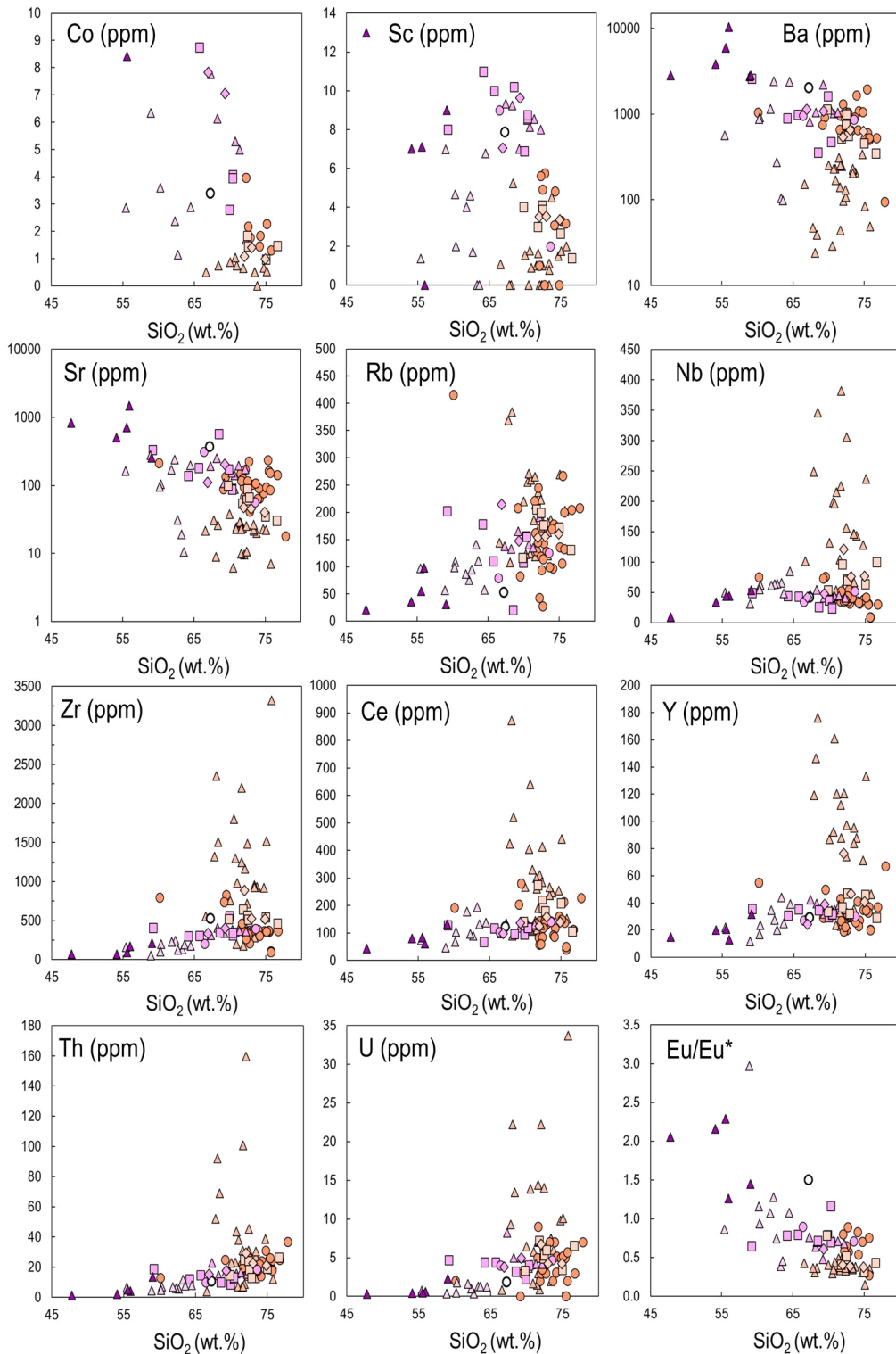


Figure 11. Harker diagrams for trace elements in Otanmäki suite granites and intermediate rocks. Symbols as in Fig. 3. Note that logarithmic scale is used for Ba and Sr.

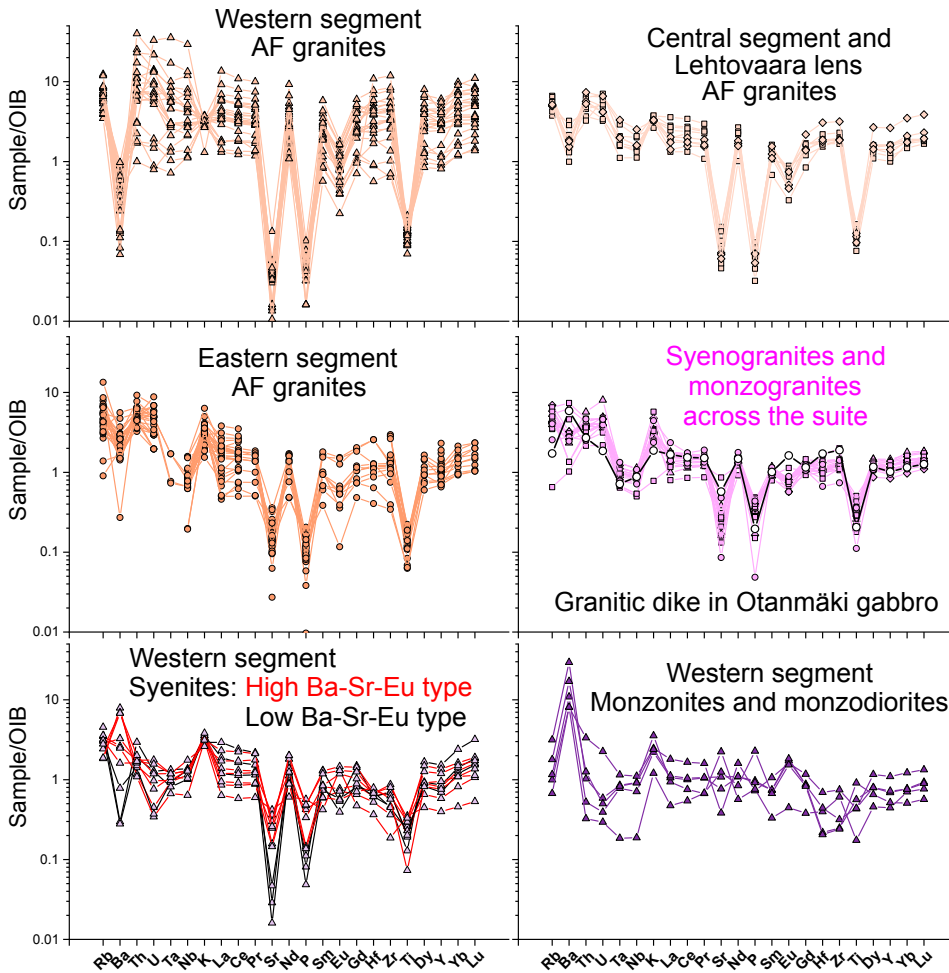


Figure 12. Ocean island basalt-normalized multi-element diagrams for Otanmäki suite granites and intermediate rocks. Normalization values are from Sun & McDonough (1989). Symbols as in Fig. 3.

overprint, the chemical compositions of the Otanmäki suite A-type rocks have remained relatively unchanged.

The crystallization temperatures for the Otanmäki suite magmas can be estimated using the modified zircon saturation index of Watson & Harrison (1983) as updated by Boehnke et al. (2013). Accordingly, the estimated temperatures at which zircon crystallized from the granitic Otanmäki suite magmas are about 850–950 °C (Fig. 14), which are comparable to magmatic temperature estimates for A-type magmas in general

(e.g., Turner et al., 1992, Patiño Douce, 1997, Frost & Frost, 2011; Scaillet et al., 2016). However, compared to the granites, the intermediate rock samples yield much lower zircon saturation temperatures falling between 650 and 850 °C (Fig. 14). The intermediate rocks have low Zr contents indicating that their parental magmas were probably zircon undersaturated, in which case the calculated temperatures would be incorrect for their initial magmatic temperatures.

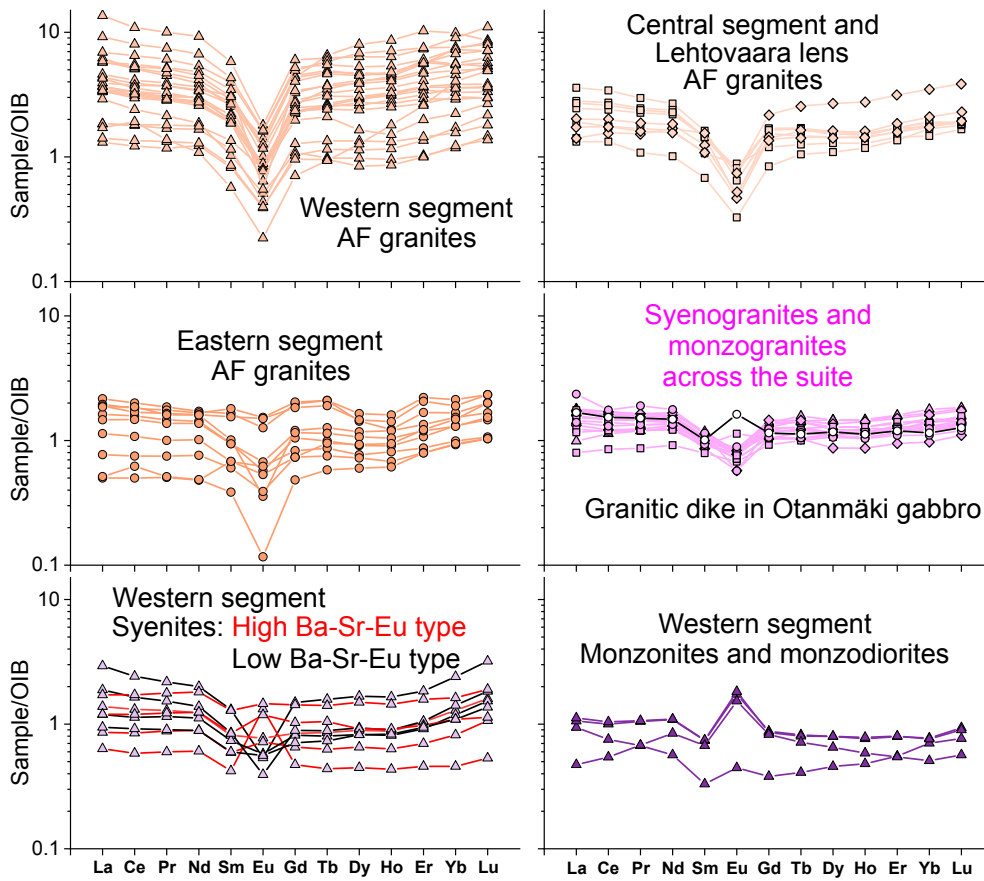


Figure 13. Ocean island basalt-normalized REE diagrams for Otanmäki suite granites and intermediate rocks. Normalization values are from Sun & McDonough (1989). Symbols as in Fig. 3.

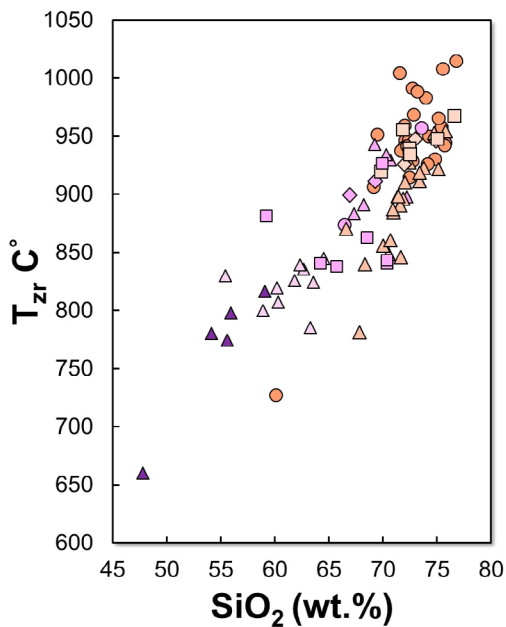


Figure 14. Zircon saturation temperature estimates shown as a function of SiO_2 for Otanmäki suite granites and intermediate rocks. T_{Zr} °C calculations based on the parametrization of Boehnke et al. (2013). Symbols as in Fig. 3.

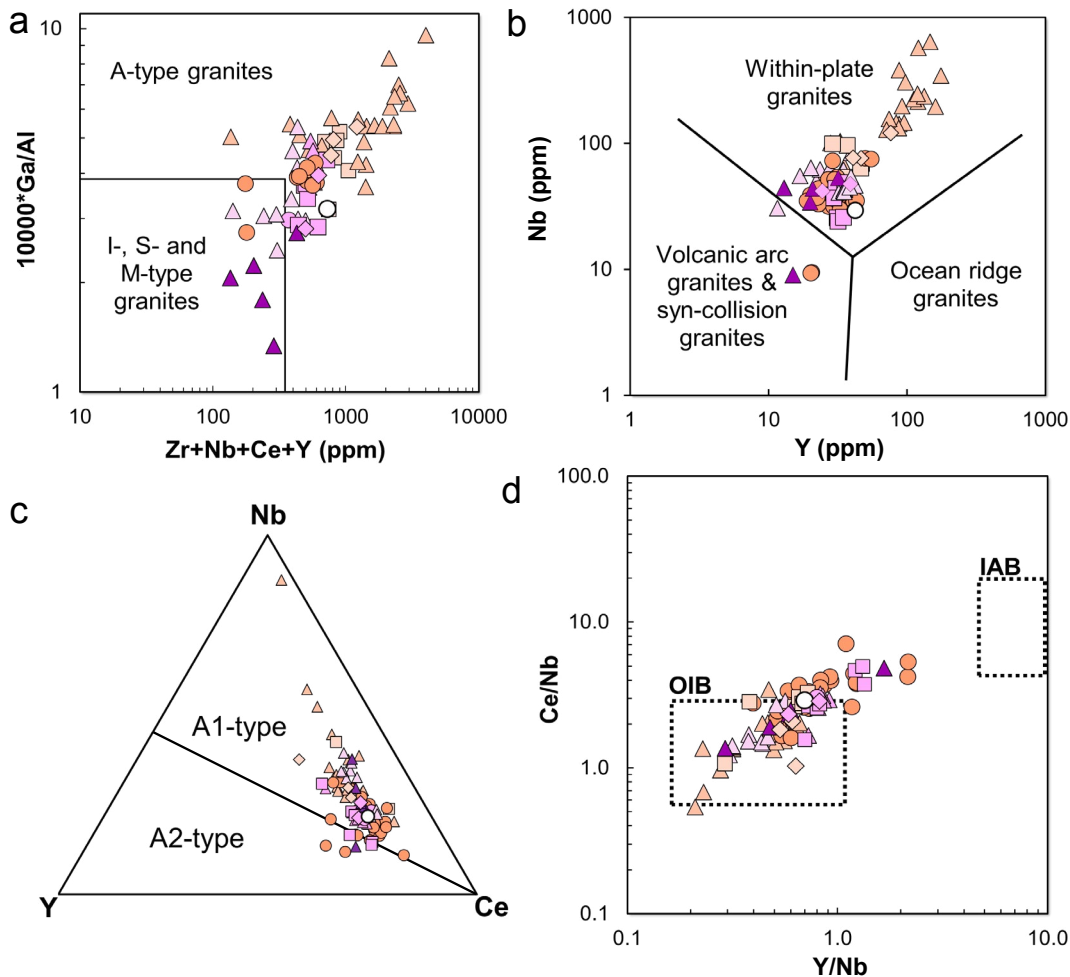


Figure 15. Tectonomagmatic discrimination diagrams for Otanmäki suite granites and intermediate rocks. (a)-(b) Trace element discrimination diagrams (Pearce et al., 1984; Whalen et al., 1987) for distinguishing A-type granites formed in within-plate settings from other types of granites. (c) Ternary diagram of Eby (1992) distinguishing between A1- and A2-type granites. (d) Ce/Nb vs. Y/Nb diagram of Eby (1990, 1992) used for defining magma source characteristics of A-type granites. OIB = ocean island basalts, IAB = island arc basalts. Symbols as in Fig. 3.

6.2 Tectonomagmatic classification

On the tectonomagmatic discriminant diagrams of Whalen et al. (1987), Pearce et al. (1984) and Eby (1990, 1992) (in Fig. 15a–c), the Otanmäki suite samples fall in the fields of within-plate and continental rift-related A1-type granites, which are commonly considered to have formed by fractionation of mafic magmas derived from ocean island basalt (OIB) type sources in rift zones (Eby, 1990, 1992). Additional evidence for the

OIB connection is shown in the Ce/Nb vs Y/Nb diagram (Fig. 15d), in which the Otanmäki suite samples exhibit trace element ratios broadly similar to those of OIBs. However, in the Th/Yb vs Nb/Yb and Th/Nb vs Nb/U diagrams (Fig. 16), the peralkaline-metaluminous granite and intermediate rock samples plot close to OIB, whereas the peraluminous granite samples plot towards the Archean granitoids (tonalite, granodiorite, granite) from the Karelia craton, indicating crustal contamination.

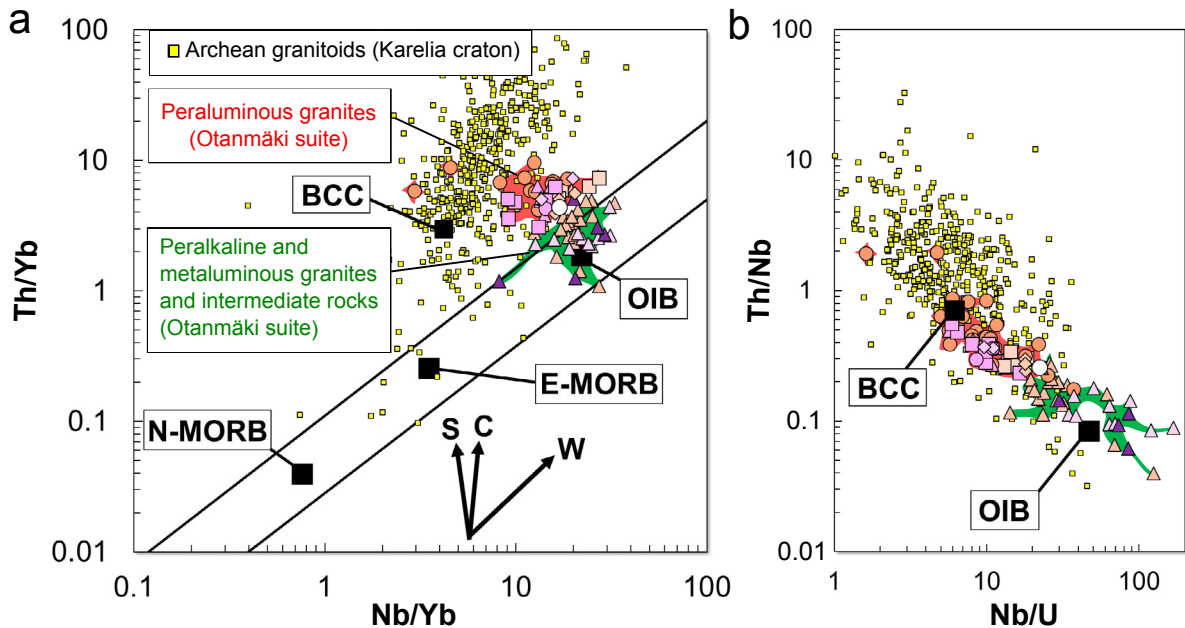


Figure 16. (a) Th/Yb vs. Nb/Yb diagram (Pearce, 2008) and (b) Th/Nb vs. Nb/U diagram for Otanmäki suite granites and intermediate rocks. OIB = ocean island basalts, E-MORB = enriched mid-ocean ridge basalts, N-MORB = normal mid-ocean ridge basalts, BCC = bulk continental crust, S = subduction component, C = crustal contamination, W = within-plate variation and fractionation. Data for basalts are from Sun & McDonough (1989) and bulk continental crust from Rudnick & Gao (2003). Archean granitoids from the Karelia craton are from Rock Geochemical Database of Finland (Rasilainen et al., 2007). Symbols as in Fig. 3.

7. Discussion

7.1 Comparison with other A-type suites

In order to better understand the A1-type signature of the Otanmäki suite, we have compared the suite with several A-type suites representing both the A1- and A2-type (Fig. 17). Eby (1992) divided granites falling in the field of within-plate and A-type granites on the diagrams of Pearce et al. (1984) and Whalen et al. (1987) into two types, A1 and A2, based on the contents of trace elements, in particular the Y/Nb ratio. The group of granites with low Y/Nb (<1.2, A1-type) includes felsic igneous rocks derived from oceanic island basalts in anorogenic settings (Eby, 1992). Granites with higher Y/Nb (A2-type) are thought to have been produced from basalts similar to those occurring

in continental margins and island arcs or by partial melting of continental crust in a wide range of tectonic settings, including collisional or anorogenic regimes (Eby, 1992).

In Figs. 17, 18 and 19, the Otanmäki suite samples are compared with samples representing examples of both A1- and A2-type suites (for details and data sources, see Electronic Appendix F1). In terms of major elements, the Otanmäki suite and the reference suites are ferroan, with the most significant differences being in the alkalinity and silica contents of the suites, as the majority of the samples representing the A1-type suites are from granitic and syenitic, peralkaline or metaluminous rocks, whereas those for the A2-type suites are mostly from metaluminous or peraluminous granites (Fig. 18). The Suomenniemi A2-type suite forms an exception as it contains small peralkaline syenitic intrusions in addition to peraluminous-

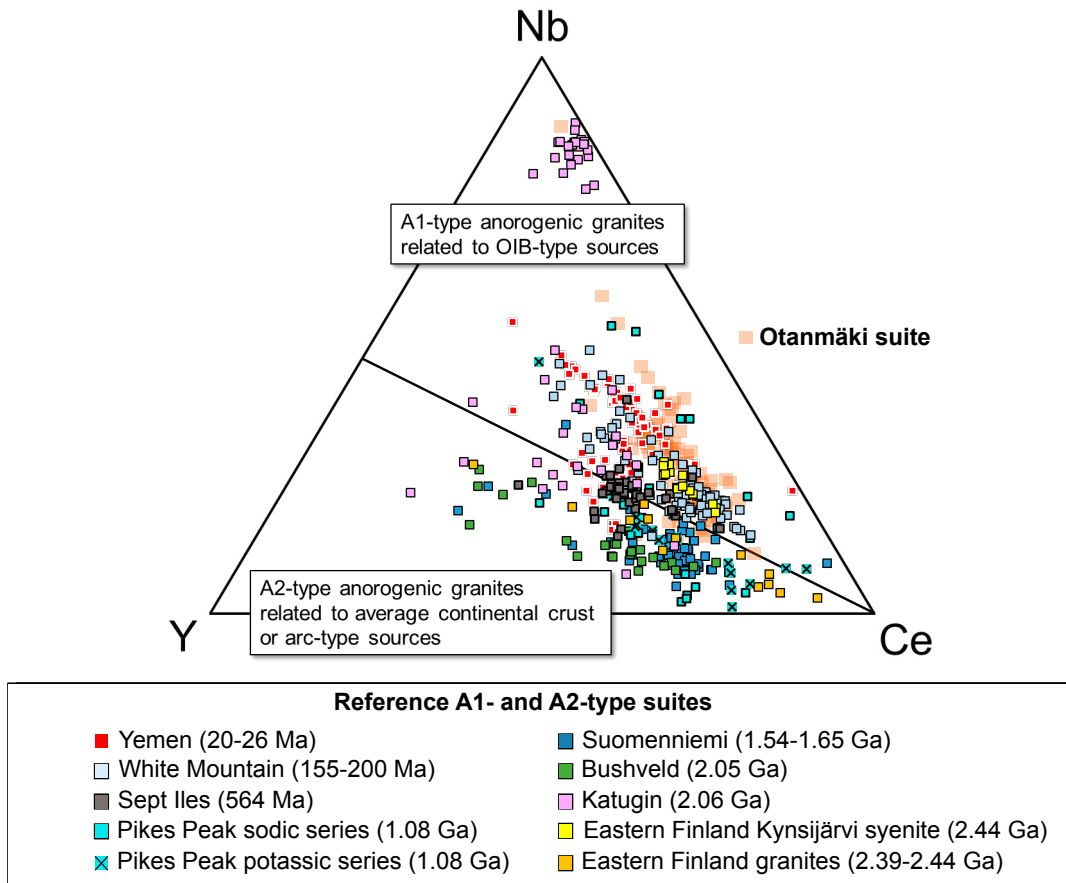


Figure 17. Samples of the Otanmäki suite and reference set of A1- and A2-type suites plotted in the Nb-Y-Ce ternary diagram of Eby (1992). Data sources for the reference A1- and A2-type suites are given in Electronic Appendix F.

metaluminoous granites (Fig. 18; Rämö, 1991). Most of the A1-type suites lack voluminous peraluminous granites, with the exception of the Yemen A1-type suite (Fig. 18).

In terms of trace elements, the Otanmäki suite shares many characteristics with A-type rocks in general, as expected, and together with the reference data they all plot in the A-type and WPG fields in plots of Pearce et al. (1984) and Whalen et al. (1987) (Fig. 18). In addition, we observed significant and systematic differences or similarities in particular in the Y/Nb, Ce/Nb and Rb/Nb ratios between the reference suites (Fig. 19). In the Otanmäki suite samples, these ratios are similar to those in the Yemen suite, White Mountain batholith, Sept Iles

granites, Katugin granites (excluding Nb-Zr-REE mineralized samples from Katugin), Kynsijärvi syenite and some components of the Pikes Peak sodic series (Fig. 19). These suites are considered to have originated by differentiation of mafic parental magmas with or without crustal assimilation, and they show OIB-like trace element characteristics, with the exception of the Sept Iles suite (Coleman et al., 1992; Eby et al., 1992, Smith et al., 1999; Lauri et al., 2006; Namur et al., 2011; Gladkochub et al., 2017; Donskaya et al., 2018). The Otanmäki suite has clearly lower Y/Nb, Ce/Nb and Rb/Nb ratios compared to the A2-type suites (Fig. 19; the Bushveld granite, rapakivi granites of the Suomenniemi batholith, potassic series granites

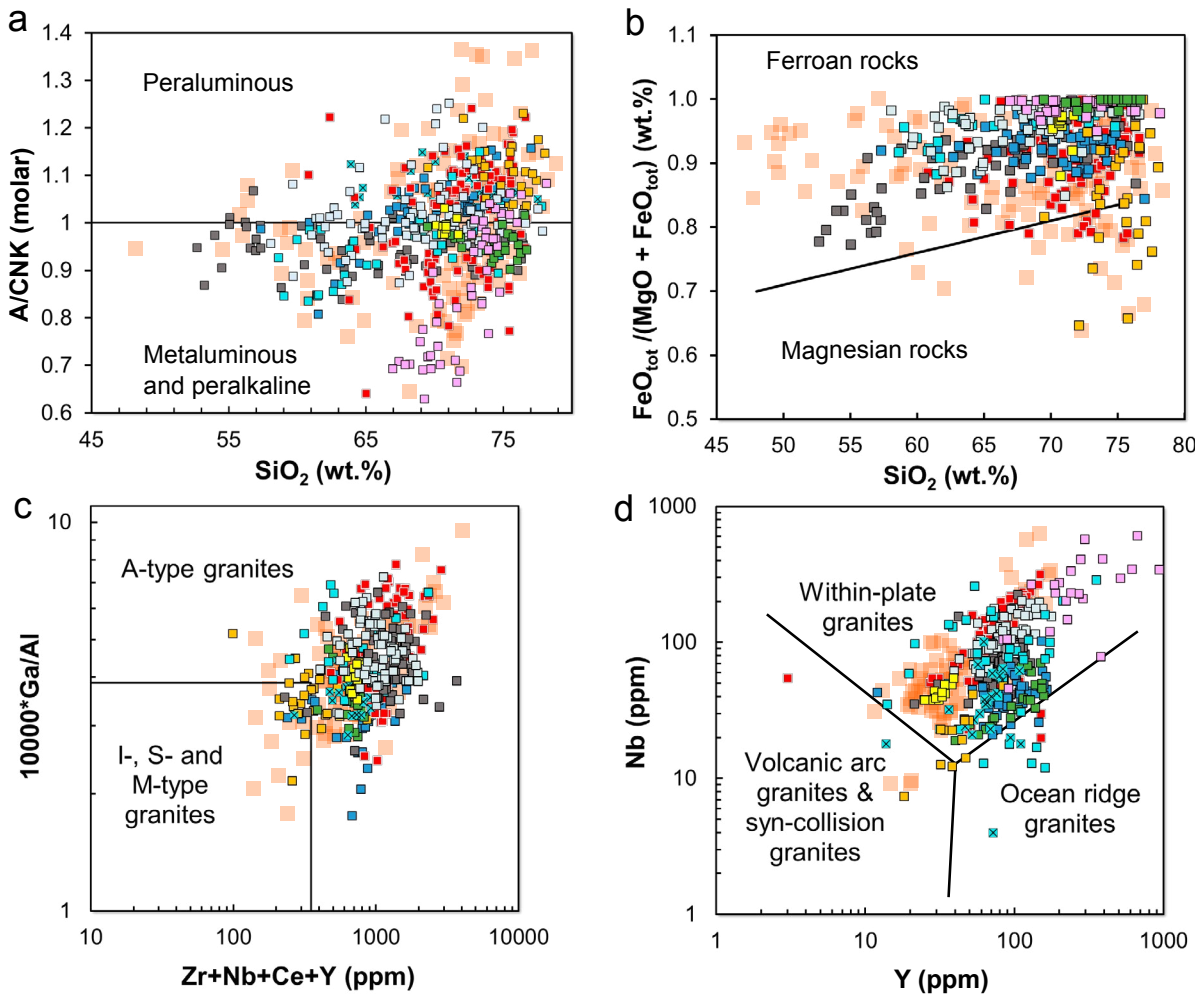


Figure 18. Samples of the Otanmäki suite and reference set of A1- and A2-type suites plotted in (a) A/CNK ($\text{Al}_2\text{O}_3/(\text{CaO} + \text{Na}_2\text{O} + \text{K}_2\text{O})$ molar) vs. SiO_2 diagram for distinguishing between peralkaline-metaluminous and peraluminous rocks, (b) $\text{FeO}_{\text{tot}}/(\text{MgO} + \text{FeO}_{\text{tot}})$ vs. SiO_2 diagram (Frost & Frost, 2008), (c) Ga/Al vs. Zr+Nb+Ce+Y diagram (Whalen et al., 1987) and (d) Nb vs. Y diagram (Pearce et al., 1984) for distinguishing A-type formed in within plate settings from other granites. Symbols and data sources as in Fig. 17. In (c), Katugin suite is missing because data for Ga were not available.

of the Pikes Peak batholith, and granite plutons of eastern Finland) considered to be derived from partial melting of felsic or intermediate igneous rocks in the continental crust and/or tholeiitic mantle-derived mafic magmas (Kleeman & Twist, 1989; Rämö, 1991; Smith et al., 1999; Mikkola et al., 2010).

Low Y/Nb ratios are typical in oceanic island, intraplate and rift zone magmas derived from OIB-type mantle sources (Eby, 1992). A high Y/

Nb ratio is common in magmas derived from arc-type sources (lithospheric mantle modified by subduction-related fluids) or in magmas derived dominantly from the continental crust, as continental crust has a high Y/Nb ratio (Eby, 1992; Rudnick & Gao, 2003; Murphy, 2007). Consequently, the A1-type suites with lower Y/Nb ratios are thought to represent differentiates of OIB-like mantle-derived melts, whereas the A2-type suites with high Y/Nb ratios are considered

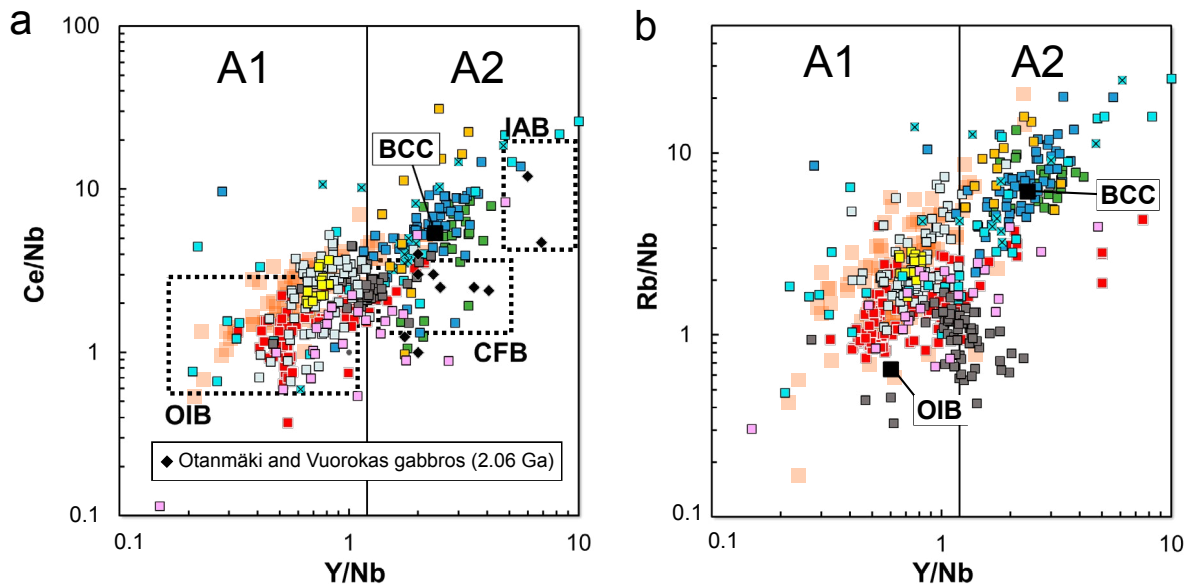


Figure 19. Samples from the Otanmäki suite and reference set of A1- and A2-type suites plotted in (a) Ce/Nb vs. Y/Nb and (b) Rb/Nb vs. Y/Nb diagrams (Eby, 1992). Reference data for bulk continental crust (BCC) are from Rudnick & Gao (2003), continental flood basalts (CFB) from Farmer (2003) and ocean island basalts from Sun & McDonough (1989). Data for the 2.06 Ga Otanmäki and Vuorokas gabbro intrusions are from Rock Geochemical Database of Finland (Rasilainen et al., 2007) and Nykänen (1995). Symbols and data sources as in Fig. 17. A1- and A2-type granites are separated by Y/Nb ratio of 1.2 (Eby, 1992).

to represent mixtures of both subcontinental lithospheric mantle (SCLM) and crust (Eby, 1992). In general, the Y/Nb ratio can be lowered in most magmas only by extensive fractionation of clinopyroxene (and/or amphibole) and raised by significant amounts of crustal assimilation (>15%) (Eby, 1992). The latter process, if extensive, can cause some gradation in the Y/Nb ratio separating the A1- to A2-types, for example, if A1-type melts become significantly contaminated with crust or incorporate material from the subduction-modified SCLM (Eby, 1992). Similarly, the Ce/Nb and Rb/Nb ratios of A-type igneous rocks serve as tracers of their sources, as these ratios are high in the continental crust or subduction-modified SCLM and low in a mantle source lacking subduction modification and in rocks derived from such mantle sources (Eby, 1992; Rudnick & Gao, 2003; Murphy, 2007).

Given the presence of intermediate rocks and the diversity of different granite types (peralkaline,

metaluminous and peraluminous) in the Otanmäki suite, it forms a rather special case. All these rocks seem to have formed in the same magmatic event, in spite of the fact that the sources of granites with such a widely varying alkalinity can be petrogenetically quite distinct (e.g., Smith et al., 1999; Shellnut & Zhou, 2007; Shellnut et al., 2009; Frost & Frost, 2011). The Otanmäki suite peralkaline-metaluminous (AF) granites and syenites are chemically similar to the rocks in the White Mountain and Pikes Peak sodic series. In both these cases, the proposed model of magma evolution involves silicic-intermediate liquids that were formed by extensive fractionation of mafic parental magmas derived from OIB-like mantle source, with only minor crustal contamination (Eby et al., 1992; Smith et al., 1999). However, the White Mountain and Pikes Peak sodic series suites lack voluminous peraluminous granite phases similar to those that are plentiful in the Otanmäki suite. It is also important to note that in the Pikes Peaks batholith, the sodic

series intrusions are accompanied by peraluminous granite intrusions of the potassic series, but these potassic series granites lack an OIB-signature and plot in the A2-type field (Figs. 17 and 19). This suggests that they have a markedly different petrogenetic history compared to the sodic series, involving partial melting of tonalitic crust (Smith et al., 1999).

Although the metaluminous granites of the Sept Iles layered intrusion belong marginally to the A1-type (Figs. 17 and 19), they only represent a poor analogue for the Otanmäki suite granites for several reasons. Firstly, unlike the Otanmäki suite A-type rocks, the granites at Sept Iles occur together with comagmatic layered troctolites, gabbros and anorthosites (Namur et al., 2011). Secondly, the Sept Iles granites lack a diversity in alkalinity, such as observed at Otanmäki (Fig. 18). The Sept Iles samples have transitional Y/Nb, Ce/Nb and Rb/Nb ratios (Fig. 19) and petrogenetic models proposed for their origin maintain that they were produced by protracted crystallization of an Fe-tholeiitic parental magma (with minimal interaction with crust) (Namur et al., 2011), not an OIB-type basalt as in case of the Otanmäki suite.

The 2.44 Ga Kynsijärvi syenite, which occurs as a dike-like intrusion (0.5 x 6 km) in the Archean basement gneisses, is also a poor analogue for the Otanmäki suite, as it only contains syenitic rocks with unusually high silica contents (~70 wt%) (Lauri et al., 2006; 2012). However, the Kynsijärvi syenites show an A1-type and OIB-like chemical signature suggesting their derivation from an enriched mantle source (Figs. 17 and 19).

Considering the chemical variation, the most identical rocks with those in the Otanmäki suite are found in the Yemen suite. The Yemen suite peralkaline to peraluminous granites, syenites and their volcanic equivalents classify dominantly as A1-type with an OIB signature, but some also plot into the A2-type field (Figs. 17–19). They are interpreted to have been generated by assimilation-fractional crystallization processes involving a parental alkali basalt magma and diverse Pan-African basement rocks as assimilants, with the

peraluminous phases of the suite representing the most and the peralkaline phases the least contaminated variants (Capaldi et al., 1987; Coleman et al., 1992; Tommasini et al., 1994; Chazot & Bertrand, 1995). A similar petrogenetic model has also been suggested for the generation of the Katugin suite of cogenetic peralkaline granites and peraluminous-metaluminous granites, but the latter with more assimilated crustal component (Donskaya et al., 2018). The most recent models proposed for the genesis of A-type rock suites also support such interpretations for the origin of peraluminous A-type granites (e.g., Shellnut et al., 2009; Frost & Frost 2011; 2013a,b; Scaillet et al., 2016) advocating that fractional crystallization of a basalt alone is not capable of generating peraluminous silicic melts, instead producing felsic or intermediate differentiates, which are either peralkaline or metaluminous depending on the starting composition (tholeiitic or alkaline), depth of differentiation and degree of crystallization (~40–60% for intermediate liquids and >80% for felsic). In contrast, the formation of peraluminous A-type granites is considered to be a consequence of either contamination of mafic magmas by quartzo-feldspathic crustal rocks or their partial melts, driving their siliceous differentiates to a more peraluminous composition (Frost & Frost, 2011) or by direct partial melting of Al-rich crustal rocks (Frost & Frost, 2011), such as common tonalites or granodiorites considered to be capable of yielding ferroan A-type first melts (e.g., Patiño Douce, 1997).

On the basis of the discussion above, we suggest that a similar combination of source components and petrogenetic processes, as have been suggested for the White Mountain, Pikes Peak sodic series, Katugin and Yemen suites, were involved in the genesis for the Otanmäki suite A-type rocks. This means that they originated primarily by differentiation of a mantle-derived mafic magma and that the generation of peraluminous granite phases likely involved a greater degree of crustal assimilation (likely of Archean granitoids) than that of the peralkaline and metaluminous granites and

intermediate rocks, which formed with only little input of material from the crust.

It appears genetically important that many of the reference granitic-syenitic A-type suites are associated with cogenetic mafic rock units (both A1- and A2-type suites; e.g., Kleeman & Twist, 1989; Rämö, 1991; Coleman et al., 1992; Eby et al., 1992; Namur et al., 2011). In the Otanmäki case, such a link could be represented by the spatially associated ca. 2.06 Ga gabbroic intrusions. However, field observations indicate that at the margins of the western segment, the 2.06 Ga gabbros and 2.05 Ga A-type rocks are separated by faults and show no evidence of intervening. Therefore, it appears that their present spatial association is due to tectonism, although it remains unresolved how much displacement (travel) the juxtaposing faulting involved. The parental magma for the 2.06 Ga gabbros is interpreted to be a Ti-V-rich evolved Fe-tholeiite (Nykänen, 1995). Such a magma is not an obvious parent for peralkaline AF granites, which are more likely derived from transitional or alkaline mafic magmas (Frost & Frost, 2011, 2013a; Scaillet et al., 2016). Also, the 2.06 Ga gabbroic rocks have Y/Nb and Ce/Nb ratios mostly similar to those of continental tholeiites, rather than those of OIBs or the Otanmäki suite A-type rocks, indicating that the 2.05 Ga A-type rocks and 2.06 Ga gabbros had different sources and thus were not cogenetic (Fig. 19). The lack of associated voluminous mafic rocks in the Otanmäki suite could be just apparent as the mafic rocks may reside at deeper levels in the crust. Actually, in some A-type suites, the amount of associated intermediate and mafic intrusive rocks increases with erosional depth (e.g., Rämö & Haapala, 2005). If this is the case in the Otanmäki suite, gravity anomalies should occur within the area of the Otanmäki-Kuluntalahti nappe, but the gravity data and maps (for gravity anomaly maps of Finland see; <https://hakku.gtk.fi/en>) indicate that neither the nappe or its surrounding units contain any large mafic masses, at least not near the surface. Alternatively, the lack of coeval mafic rocks could be explained by the allochthonous nature of the Otanmäki suite, in which case the nappes could

represent long-travelled thrust slivers, which have been detached from their root area where related mafic rocks may have resided (see discussion in section 7.3).

Our review of literature suggests that in contrast to A2-type suites, early Paleoproterozoic (2.0–2.5 Ga) examples of A1-type suites with an OIB-like chemical signature are globally extremely rare (see Electronic Appendix F2–4), which is astonishing considering the large number of studies conducted on A-type suites worldwide (e.g., Bonin, 2007; Dall’Agnol et al., 2012; Grebennikov, 2014 and references therein). In comparison to the 2.05 Ga Otanmäki suite, most of the recorded A1-type suites (including granites and intermediate rocks and/or their volcanic equivalents) are mostly considerably younger (<1.0 Ga; see Electronic Appendix F4), with only few being older (2.44 Ga; Lauri et al., 2012; and 2.7–2.6 Ga; Zozulya et al., 2005 and references therein), and only one being similar in age (the 2.06 Ga Katugin suite, southern Siberia; Gladkochub et al., 2017; Donskaya et al., 2018). The recorded examples are located mostly in within-plate settings (oceanic or continental), either in hotspots, rift belts or triple junctions near divergent boundaries of lithospheric plates.

7.2 Tectonic setting of the Otanmäki suite

The post-Archean evolution of the Karelia craton involved a period of tectonic quiescence with minimal or no recorded accretional/collisional processes from ca. 2.45 to 2.10 Ga (Hanski & Melezhik, 2013b). During this period, there was significant erosion and peneplanization of the Karelia continent but also several discrete episodes of crustal extension resulting in opening of intracontinental rift basins (Laajoki, 2005; Vuollo & Huhma, 2005; Lahtinen et al., 2005; Hanski & Melezhik, 2013a,b). The rifting episodes were associated with mafic magmatism involving repeated mafic dike swarm episodes (and associated shallow level sills) and emplacement of intrusions and extrusive rocks at ca. 2.5, 2.45, 2.4, 2.2 and

2.15 Ga (Vuollo & Huhma 2005; Hanski, 2013; Huhma et al., 2018). However, the rifting during these stages did not progress to continental break-up (Lahtinen et al., 2015).

The 2.1–2.05 Ga stage is interpreted to represent the main rifting of the Karelia continent and eventually led to the final break-up and separation of the Karelia craton along its southwestern margin (Lahtinen et al., 2015). At ca. 2.1 Ga, large areas of the Karelia craton were affected by voluminous mafic magmatism as exemplified by the widespread occurrence Fe-tholeiitic dike swarms in eastern Finland and adjacent Russia connected to a 2.1 Ga mantle plume (Vuollo & Huhma, 2005, Hanski 2013; Huhma et al., 2018). In addition, rare felsic plutonic rocks 2.1 Ga in age are found in northern Finland and are believed to have been formed by crustal melting caused by extensive mafic underplating and heating in the craton (Ahtonen et al., 2007). A significant magmatic event also occurred at 2.06–2.05 Ga as there are signs of 2.05 Ga mafic dike swarms in northern Finland and 2.06–2.05 Ga mafic intrusions in northern and central Finland (Vuollo & Huhma, 2005; Huhma et al., 2018). In addition, there are 2.06 Ga alkaline mafic to felsic volcanic units (Kuetsjärvi Volcanic Formation) in the Pechenga belt in the Kola Peninsula, Russia (Melezhik & Hanski, 2013) and in northern and central Finland (the latter discussed further in a section further). Originally, the Kola Peninsula represents a separate Archean craton, but its Paleoproterozoic evolution involves a very similar history to that of the Karelia craton with ca. 2.4–2.1 Ga rifting episodes and break-up probably after 2.1 Ga (Daly et al., 2006). It is considered that the Kola craton docked with the Karelia craton during the Lapland-Kola orogeny at ca. 1.93–1.91 Ga (Daly et al., 2006) and before that they formed separate cratons distant from each other or alternatively were located in the opposite sides of a large supercontinent that separated at ca. 2.1–2.05 Ga (Lahtinen et al., 2005; Daly et al., 2006).

With these constraints from the rock record indicating craton-wide extension and mantle-

upwelling during 2.1–2.05 Ga, the pre-Svecofennian emplacement age (2050 ± 2 Ma) and A1-type chemistry of the Otanmäki suite is intriguing in a geotectonic sense for the entire Fennoscandian Shield. The Otanmäki suite rocks seem to record a rare occurrence A-type felsic-intermediate plutonism related to the 2050 Ma continental rifting event, which could have led to the disintegration of the Archean Karelia continent. This hypothesis is consistent with the present location of the Otanmäki suite only few tens of kms east of the present-day Karelia-Svecofennia boundary in the same thrust belt with the 1.95 Ga Jormua ophiolite complex. The Jormua ophiolite, with its crustal part predating the Svecofennian collision by ca. 50 Ma, has several features in common with continental margin ophiolites, such as the Ligurian ophiolites generated during the opening of the Tethys (Kontinen, 1987; Peltonen et al., 1996, 1998; Peltonen & Kontinen, 2004). Given the break-up/extension affinity of both the Otanmäki suite and Jormua ophiolite, Peltonen et al. (1996) proposed that both were generated in later stages of the break-up of the Karelia craton, spatially somewhere “westwards” of the present Kainuu schist belt and in time between ca. 1.97–1.95 Ga. However, as we now know that the Otanmäki suite A-type rocks emplaced 100 Ma earlier, a revision of the earlier model of Peltonen et al. (1996) is needed.

Rocks dated at ca. 2.05 Ga are rare along the margin of the Karelia craton; in addition to the Otanmäki-Kuluntalahti nappe and Lehtovaara lens, only two other occurrences in northern and central Finland are presently known. Both of these occurrences are located in Paleoproterozoic supracrustal belts (Peräpohja and Siilinjärvi belts) and they contain small units of ca. 2.05–2.06 Ga A-type felsic, either subvolcanic or effusive rocks (Perttunen & Vaasjoki, 2001; Lukkarinen, 2008). Lahtinen et al. (2015) have interpreted that these 2.05–2.06 Ga felsic volcanic-subvolcanic rocks and the 2.05 Ga Otanmäki suite represent rifting that led to the break-up of the Karelia craton at ca. 2.05 Ga. For the 1.95 Ga ophiolites, Lahtinen et al. (2015) proposed that they record a 100-Ma-

later episode of extension and generation of a screen of oceanic crust within the since ca. 2.06 Ga formed continental margin. As this complicated model of two break-up events/oceanizations lacks documented evidence from the sedimentary rock record, we agree with the proposal of Peltonen et al. (1996) and suggest that the Otanmäki suite marks the onset (initiation) of the break-up process and the oceanic crust of the Jormua ophiolite generated in a rift-to-drift transition stage. The new age data show that the rifting process was sluggish, lasting ca. 100 Ma. Similarly, a slow extension-rifting-opening episode has been established between Greenland and Eurasia, with pulses of extension/rifting occurring since at least early Cretaceous (144 Ma) but the true break-up not before Oligo-Miocene (33–25 Ma) (Roberts et al., 1999; Lundin & Dore, 2005). The Svecofennian collisional event, which is usually inferred to have initiated at ca. 1.90 Ga, implies that the Karelia margin had a relatively short life-span of ca. 50 Ma.

There are two potential explanations for the restriction of the Otanmäki suite A-type rocks to the two tectonic sheet- and lens-like bodies in which it now occurs: (1) the A-type granites and intermediate rocks were emplaced as a relatively narrow chain of plutons between the Archean complexes presently surrounding the Otanmäki suite nappe and lens, or (2) they are long-travelled thrust slices from a now buried or removed outer (more “westerly”) part of the Karelia craton margin. The first option requires imbricate shortening with wedge losses between the Archean complexes to explain the present tectonic contacts. The second option assumes detachment and eastwards thrusting of a sheet of A-type granites and intermediate rocks from a more westerly part of the craton margin, and stacking it into a position between the Archean complexes now in the north and south. In both cases, later strike-slip tectonism cutting along the Karelia-Svecofennia collisional zone contributed significantly to the final tectonic pattern, rotating and displacing the Otanmäki suite A-type granite and intermediate rock bodies anticlockwise along with the flanking Archean gneiss complexes.

Based on the present data, we consider the simpler model involving parautochthonous status more likely, but the case still remains open. A potential resolution to the problem could be obtained by dating the TTG rocks occurring within the A-type rocks in the western segment (Luodesuo enclave) of the Otanmäki-Kuluntalahti nappe and/or the strained metagabbroic-leucodioritic gneisses that occur within the northern margin of the nappe (Kemiläistenräme and Vuorijärvi mafic rocks), to find out whether they correlate or not with the gneisses in the surrounding Archean complexes. It would also be useful to know whether the A-type granite dikes cutting the 2.06 Ga gabbro intrusions at Otanmäki are 2.05 Ga or not in age. The positive case would favor a parautochthonous tectonic status of the Otanmäki-Kuluntalahti nappe. Also, the volcanic-sedimentary rocks intruded by the 2.05 Ga A-type granites within the Otanmäki-Kuluntalahti nappe and Lehtovaara lens should be studied, as these rocks appear similar to rocks in the Jatulian and Lower Kalevian sequences in the main Kainuu schist belt. If correlation is demonstrated, it would favor the parautochthonous interpretation for the Otanmäki suite, but it is also possible that these rocks represent slices detached from cratonic and rift sequences related to putative, now buried (below Svecofennian crust) or away drifted outer parts of the pre-1.9 Ga craton margin. In addition, we already know that some of the metasedimentary enclaves within the Otanmäki-Kuluntalahti nappe and Lehtovaara lens incorporate rocks, such as conglomerates and cobbles-boulders in them, which do not have counterparts or obvious sources elsewhere in the regional rock record. Whatever the outcomes of such future studies are, they will be important for understanding the evolution of the Karelia craton margin.

8. Conclusions

The following conclusions can be drawn:

1. The Otanmäki suite comprises a broad variety of gneissic A-type felsic and intermediate igneous rocks including monzodiorites, monzonites, syenites and peralkaline to peraluminous granites, not just alkaline granites as was previously thought. Both deeply emplaced plutonic and shallowly emplaced subvolcanic variants are present. The new U-Pb zircon ages obtained for granitic members and considered to date the magmatism fall in the range of 2040 to 2060 Ma, including a precise age of 2050 ± 2 Ma. The ca. 2050 Ma age demonstrates that these rocks represent a rare occurrence of pre-orogenic felsic to intermediate plutonism in the Karelia craton, formed ca. 150 Ma before the start of the Svecofennian orogeny, during which they were metamorphosed and deformed.
2. Geochemically, the Otanmäki suite granites and related intermediate rocks classify as A1-type, exhibiting similar chemical characteristics to other A1-type suites thought to be generated by differentiation of mantle-derived mafic melts with or without crustal interaction. Rocks of similar composition and age seem to be missing elsewhere in Finland, and even globally, the recorded counterparts of such an old age are rare.
3. Tectonically, the Otanmäki suite granites and intermediate rocks occur as two tectonic units (nappes) located between Archean granitoid gneiss complexes, Paleoproterozoic supracrustal units and the 1.95 Ga Jormua ophiolite complex close to the Karelia craton margin in central Finland. The questions of the original geologic setting and paleogeographic position of the Otanmäki suite A-type rocks remain debatable, but the presence of supracrustal rocks in the Otanmäki suite nappes that are similar to those in cratonic platformal and rift

deposits in the Kainuu schist belt suggest a parautochthonous nature. However, due to the restriction of the A-type rocks to the two nappes together with supracrustal rocks potentially only occurring in the Otanmäki suite nappes and the lack of temporally and spatially associated mafic rock units, an allochthonous nature of the suite can neither be completely discarded.

4. The age, A1-type chemical affinity, and the present location of the Otanmäki suite close to the Karelia craton margin indicates that the A-type granites and related intermediate rocks were generated in the early stages of lithospheric break-up of the Karelia craton at ca. 2050 Ma. It seems that their emplacement marks the start of the apparently very slow process of extension-rifting that finally led to the complete break-up of the Karelia craton, possibly at 1.95 Ga when the Jormua ophiolite was formed.

Acknowledgements

Financial support for this study was provided by the Advanced Materials Doctoral Programme (ADMA-DP) of the University of Oulu, K.H. Renlund Foundation and Tauno Tönning Foundation. The field work was profoundly supported by Otanmäki Mine Oy (www.otanmaki.fi) and Jouko Jylänki, the CEO of the company, which is gratefully acknowledged. Hugh O'Brien, Yann Lahaye, Leena Järvinen, Lasse Heikkinen, and Jenni Keränen are acknowledged for laboratory assistance. Asko Käpyaho and Gregory Shellnut are thanked for their constructive comments that helped to improve this manuscript.

Supplementary data

Electronic Appendices A–F for this article are available via Bulletin of the Geological Society of Finland web page.

References

- Ahtonen, N., Hölttä, P. & Huhma, H., 2007. Intracratonic Palaeoproterozoic granitoids in northern Finland: prolonged and episodic crustal melting events revealed by Nd isotopes and U-Pb ages on zircon. *Bulletin of the Geological Society of Finland* 79, 143–174.
<https://doi.org/10.17741/bgsf/79.2.002>
- Boehnke, P., Watson, B.E., Trail, D., Harrison, M.T. & Schmitt, A.K., 2013. Zircon saturation re-visited. *Chemical Geology* 351, 324–334.
<https://doi.org/10.1016/j.chemgeo.2013.05.028>
- Bonin, B., 2007. A-type granites and related rocks: Evolution of a concept, problems and prospects. *Lithos* 97, 1–29.
<https://doi.org/10.1016/j.lithos.2006.12.007>
- Capaldi, G., Chiesa, S., Manetti, P., Orsi, G. & Poli, G., 1987. Tertiary anorogenic granites of the western border of the Yemen Plateau. *Lithos* 20, 433–444.
[https://doi.org/10.1016/0024-4937\(87\)90028-4](https://doi.org/10.1016/0024-4937(87)90028-4)
- Chazot, G. & Bertrand, H., 1995. Genesis of silicic magmas during tertiary continental rifting in Yemen. *Lithos* 36, 69–83.
[https://doi.org/10.1016/0024-4937\(95\)00012-5](https://doi.org/10.1016/0024-4937(95)00012-5)
- Coleman, R.G., DeBari, S. & Peterman, Z., 1992. A-type granite and the Red Sea opening. *Tectonophysics* 204, 27–40.
[https://doi.org/10.1016/0040-1951\(92\)90267-A](https://doi.org/10.1016/0040-1951(92)90267-A)
- Dall'Agnol, R., Frost, C.D. & Rämö T., 2012. IGCP Project 510 “A-type granites and related rocks through time”: Project vita, results, and contribution to granite research. *Lithos* 151, 1–16.
<https://doi.org/10.1016/j.lithos.2012.08.003>
- Daly, J.S., Balagansky V.V., Timmerman M.J. & Whitehouse, M.J., 2006. The Lapland-Kola orogen: Palaeoproterozoic collision and accretion of the northern Fennoscandian lithosphere. In: Gee, D.G., Stephenson, R.A. (eds.), *European Lithosphere Dynamics*, 32nd ed. Geological Society Memoir, London, pp. 579–598.
<https://doi.org/10.1144/GSL.MEM.2006.032.01.35>
- Donskaya, T.V., Gladkochub, D.P., Sklyarov, E.V., Kotov, A.B., Larin, A.M., Starikova, A.E., Mazukabzov, A.M., Tolmacheva, E.V. & Velikoslavinskii, S.D., 2018. Genesis of the Paleoproterozoic rare-metal granites of the Katugin Massif. *Petrology* 26, 52–71.
<https://doi.org/10.1134/S0869591118010022>
- Eby, G.N., 1990. The A-type granitoids: a review of their occurrence and chemical characteristics and speculations on their petrogenesis. *Lithos* 26, 115–134.
[https://doi.org/10.1016/0024-4937\(90\)90043-Z](https://doi.org/10.1016/0024-4937(90)90043-Z)
- Eby, G.N., 1992. Chemical subdivision of the A-type granitoids: Petrogenetic and tectonic implications. *Geology* 20, 641–644.
[https://doi.org/10.1130/0091-7613\(1992\)020<0641:CSOTAT>2.3.CO;2](https://doi.org/10.1130/0091-7613(1992)020<0641:CSOTAT>2.3.CO;2)
- Eby, G.N., Krueger, H.W. & Creasy, J.W., 1992. Geology, geochronology, and geochemistry of the White Mountain batholith, New Hampshire. In: Puffer, J.H., Ragland, P.C. (eds.), *Eastern North American Mesozoic Magmatism*. Geological Society of America, Special Paper 268, 379–397.
<https://doi.org/10.1130/SPE268-p379>
- Elo, S., 1997. Interpretations of the gravity anomaly map of Finland. *Geophysica* 33, 51–80.
- Farmer, G.L., 2003. Continental basaltic rocks. In: Rudnick, R.L. (ed.), *The Crust*. Treatise on Geochemistry, Volume 3. Elsevier-Pergamon, Oxford, pp. 85–121.
<https://doi.org/10.1016/B0-08-043751-6/03019-X>
- Frost, B.R. & Frost, C.D., 2008. A geochemical classification for feldspathic igneous rocks. *Journal of Petrology* 49, 1955–1969.
<https://doi.org/10.1093/petrology/egn054>
- Frost, C.D. & Frost, B.R., 2011. On ferroan (A-type) granitoids: their compositional variability and modes of origin. *Journal of Petrology* 52, 39–53.
<https://doi.org/10.1093/petrology/egq070>
- Frost, C.D. & Frost, B.R., 2013a. Proterozoic ferroan feldspathic magmatism. *Precambrian Research* 228, 151–163.
<https://doi.org/10.1016/j.precamres.2013.01.016>
- Frost, B.R. & Frost, C.D., 2013b. *Essentials of Igneous and Metamorphic Petrology*. Cambridge University Press, New York, 314 p.
- Gaal, G., 1990. Tectonic styles of early Proterozoic ore deposition in the Fennoscandian Shield. *Precambrian Research* 46, 83–114.
[https://doi.org/10.1016/0301-9268\(90\)90068-2](https://doi.org/10.1016/0301-9268(90)90068-2)
- Gladkochub, D.P., Donskaya, T.V., Sklyarov, E.V., Kotov, A.B., Vladykin, N.V., Pisarevsky, S.A., Larin, M.A., Salnikova, E.B., Saveleva, V.B., Sharygin, V.V., Starikova, A.E., Tolmacheva, E.V., Velikoslavinsky, S.D., Mazukabzov, A.M., Bazarova, E.P., Kovach, V.P., Zagornaya, N.Y., Alymova, N.V. & Khromova, E.A., 2017. The unique Katugin rare-metal deposit (southern Siberia): constraints on age and genesis. *Ore Geology Reviews* 91, 246–263.
<https://doi.org/10.1016/j.oregeorev.2017.10.002>
- Grebennikov, A.V., 2014. A-type granites and related rocks: petrogenesis and classification. *Russian Geology and Geophysics* 55, 1074–1086.
<https://doi.org/10.1016/j.rgg.2014.08.003>
- Hanski, E.J., 2013. Evolution of the Paleoproterozoic (2.50–1.95 Ga) non-orogenic magmatism in the eastern part of the Fennoscandian Shield. In: Melezhik, V.A., Prave, A.R., Hanski, E.J., Fallick, A.E., Lepland, A., Kump, L.R., Strauss, H. (eds.), *Reading the Archive of Earth's Oxygenation*, Volume 1, The Palaeoproterozoic of Fennoscandia as Context for the Fennoscandian Arctic Russia – Drilling Early Earth Project, Springer-Verlag, Berlin, Heidelberg, pp. 179–244.
https://doi.org/10.1007/978-3-642-29682-6_6
- Hanski, E.J. & Melezhik, V.A., 2013a. Litho- and chronostratigraphy of the Palaeoproterozoic Karelian formations. In:

- Melezhik, V.A., Prave, A.R., Hanski, E.J., Fallick, A.E., Lepland, A., Kump, L.R., Strauss, H. (eds.), Reading the Archive of Earth's Oxygenation, Volume 1, The Palaeoproterozoic of Fennoscandia as Context for the Fennoscandian Arctic Russia – Drilling Early Earth Project. Springer-Verlag, Berlin, Heidelberg, pp. 39–110.
https://doi.org/10.1007/978-3-642-29682-6_4
- Hanski, E.J. & Melezhik, V.A., 2013b. Palaeotectonic and Palaeogeographic Evolution of Fennoscandia in the Early Palaeoproterozoic. In: Melezhik, V.A., Prave, A.R., Hanski, E.J., Fallick, A.E., Lepland, A., Kump, L.R., Strauss, H. (eds.), Reading the Archive of Earth's Oxygenation, Volume 1, The Palaeoproterozoic of Fennoscandia as Context for the Fennoscandian Arctic Russia – Drilling Early Earth Project, Springer-Verlag, Berlin, Heidelberg, pp. 111–178.
https://doi.org/10.1007/978-3-642-29682-6_5
- Hölttä, P., Heilimo, E., Huhma, H., Juopperi, H., Kontinen, A., Konnunaho, H., Lauri, L., Mikkola, P., Paavola, J. & Sorjonen-Ward, P. 2012a. Archaean complexes of the Karelia Province in Finland. Geological Survey of Finland, Special Paper 54, 9–20.
- Hölttä, P., Heilimo, E., Huhma, H., Kontinen, A., Mertanen, S., Mikkola, P., Paavola, J., Peltonen, P., Semprich, J., Slabunov, A. & Sorjonen-Ward, P. 2012b. The Archaean of the Karelia Province in Finland. Geological Survey of Finland, Special Paper 54, 21–73.
- Huhma, H., O'Brien, H., Lahaye, Y. & Mänttari, I., 2011. Isotope geology and Fennoscandian lithosphere evolution. In: Nenonen, K., Nurmi, P.A. (eds.), Geoscience for Society, 125th Anniversary Volume. Geological Survey of Finland, Special Paper 49, 35–48.
- Huhma, H., Hanski, E., Kontinen, A., Vuollo, J., Mänttari, I. & Lahaye, Y., 2018. Sm–Nd and U–Pb isotope geochemistry of the Paleoproterozoic mafic magmatism in eastern and northern Finland. Geological Survey of Finland, Bulletin 405, 150 p.
- Hytönen, K. & Hautala, T., 1985. Aegirine and riebeckite of the alkali gneiss of Pikkukallio in the Honkamäki–Otanmäki region, Finland. Bulletin of the Geological Society of Finland 57, 169–180.
<https://doi.org/10.17741/bgsf/57.1-2.014>
- Iljina, M. & Hanski, E., 2005. Layered mafic intrusions of the Tornio–Näränkävaara belt. In: Lehtinen, M., Nurmi, P., Rämö, O. T. (eds.), Precambrian Bedrock of Finland – Key to the Evolution of the Fennoscandian Shield. Elsevier Science B.V., Amsterdam, pp. 103–138.
[https://doi.org/10.1016/S0166-2635\(05\)80004-0](https://doi.org/10.1016/S0166-2635(05)80004-0)
- Kärenlampi, K., Paulick, H., Hanski, E., Pohjolainen, E., Kontinen, A., Huhma, H. & Jylänki, J., 2017. The Otanmäki rare metal (Nb, Zr, REE) mineralization, central Finland. Mineral Resources to Discover, Proceedings of the 14th SGA Biennial Meeting, Volume 4, 1357–1360.
- Kleemann, G.J. & Twist, D., 1989. The compositionally-zoned sheet-like granite pluton of the Bushveld Complex: evidence bearing on the nature of A-type magmatism. Journal of Petrology 30, 1383–1414.
<https://doi.org/10.1093/ptrology/30.6.1383>
- Koistinen, T., 1981. Structural evolution of an early Proterozoic stratabound Cu–Co–Zn deposit, Outokumpu, Finland. Transactions of the Royal Society of Edinburgh, Earth Sciences 72, 115–158.
<https://doi.org/10.1017/S0263593300009949>
- Kontinen, A., 1987. An Early Proterozoic ophiolite–the Jormua mafic-ultramafic complex, northeastern Finland. Precambrian Research 35, 313–341.
[https://doi.org/10.1016/0301-9268\(87\)90061-1](https://doi.org/10.1016/0301-9268(87)90061-1)
- Kontinen, A., 2002. Palaeoproterozoic tectonothermal overprint in the Eastern Finland Archaean Complex and some thoughts of its tectonic setting. In: Korsman, K., Lestinen, P. (eds.), Raahe-Laatokka Symposium, Extended Abstracts. Geological Survey of Finland, Report K21.42/2002/1, pp. 42–62.
- Kontinen, A. & Paavola, J., 2006. A preliminary model of the crustal structure of the Eastern Finland Archaean Complex between Vartiuss and Vieremä, based on constraints from surface geology and FIRE 1 seismic survey. Geological Survey of Finland, Special Paper 43, 223–240.
- Kontinen, A. & Hanski, E., 2015. The Talvivaara black shale-hosted Ni–Zn–Cu–Co deposit in eastern Finland. In: Maier, W. D., Lahtinen, R., O'Brien, H. (eds.), Minerals Deposits of Finland. Elsevier, Amsterdam, pp. 557–612.
<https://doi.org/10.1016/B978-0-12-410438-9.00022-4>
- Kontinen, A., Paavola, J. & Lukkarinen, H., 1992. K–Ar ages of hornblende and biotite from Late Archaean rocks of eastern Finland – interpretation and discussion of tectonic implications. Geological Survey of Finland, Bulletin 365, 31 p.
- Kontinen, A., Huhma, H., Lahaye, Y. & O'Brien, H., 2013a. New U–Pb zircon age, Sm–Nd isotope and geochemical data for Otanmäki suite granites in the Kainuu area, Central Finland. In: Hölttä, P. (ed.), Current Research: GTK Mineral Potential Workshop, Kuopio, May 2012. Geological Survey of Finland, Report of Investigation 198, 65–69.
- Kontinen, A., Huhma, H., Lahaye, Y. & O'Brien, H., 2013b. New U–Pb zircon age, Sm–Nd isotope and geochemical data on Proterozoic granitic rocks in the area west of the Oulunjärvi lake, central Finland. In: Hölttä, P. (ed.), Current Research: GTK Mineral Potential Workshop, Kuopio, May 2012. Geological Survey of Finland, Report of Investigation 198, 70–74.
- Kontinen, A., Huhma, H., Lahaye, Y., O'Brien, H. & Torppa, A., 2013c. Shoshonitic and alkaline 1.86–1.85 Ga magmatism at the contact of the Svecofennian and Karelian domains in the Pyhäntä area, central Finland. In: Hölttä, P. (ed.), Current Research: GTK Mineral Potential Workshop, Kuopio, May 2012. Geological Survey of Finland, Report of Investigation 198, 75–79.
- Korsman, K., Korja, T., Pajunen, M. & Virransalo, P., 1999.

- The GGT/SVEKA transect; structure and evolution of the continental crust in the Paleoproterozoic Svecofennian orogen in Finland. *International Geology Review* 41, 287–333.
<https://doi.org/10.1080/00206819909465144>
- Kuivasaari, T., Torppa, A., Äikäs, O. & Eilu, P., 2012. Otanmäki V-Ti-Fe. In: Eilu, P. (ed.), *Mineral Deposits and Metallogeny of Fennoscandia*. Geological Survey of Finland, Special Paper 53, 284–286.
- Laajoki, K., 2005. Karelian supracrustal rocks. In: Lehtinen, M., Nurmi, P., Rämö, T. (eds.), *The Precambrian Bedrock of Finland – Key to the Evolution of the Fennoscandian Shield*. Elsevier Science B.V., Amsterdam, pp. 279–342.
[https://doi.org/10.1016/S0166-2635\(05\)80008-8](https://doi.org/10.1016/S0166-2635(05)80008-8)
- Lahtinen, R., Korja, A. & Nironen, M., 2005. Palaeoproterozoic tectonic evolution of the Fennoscandian Shield. In: Lehtinen, M., Nurmi, P., Rämö, T. (eds.), *The Precambrian Bedrock of Finland – Key to the Evolution of the Fennoscandian Shield*. Elsevier Science B.V., Amsterdam, pp. 418–532.
[https://doi.org/10.1016/S0166-2635\(05\)80012-X](https://doi.org/10.1016/S0166-2635(05)80012-X)
- Lahtinen, R., Huhma, H., Kontinen, A., Kohonen, J. & Sorjonen-Ward, P., 2010. New constraints for the source characteristics, deposition and age of the 2.1–1.9 Ga metasedimentary cover at the western margin of the Karelian Province. *Precambrian Research* 176, 77–93.
<https://doi.org/10.1016/j.precamres.2009.10.001>
- Lahtinen, R., Huhma, H., Lahaye, Y., Kousa, J. & Luukas, J., 2015. Archean–Proterozoic collision boundary in central Fennoscandia: Revisited. *Precambrian Research* 261, 127–165.
<https://doi.org/10.1016/j.precamres.2015.02.012>
- Lauri, L.S., Rämö, O.T., Huhma, H., Mänttari, I. & Räsänen, J., 2006. Petrogenesis of silicic magmatism related to the ~2.44 Ga rifting of Archean crust in Koillismaa, eastern Finland. *Lithos* 86, 137–166.
<https://doi.org/10.1016/j.lithos.2005.03.016>
- Lauri, L.S., Mikkola, P. & Karinen, T., 2012. Early Paleoproterozoic felsic and mafic magmatism in the Karelian province of the Fennoscandian shield. *Lithos* 151, 74–82.
<https://doi.org/10.1016/j.lithos.2012.01.013>
- Lindholm, O. & Anttonen, R., 1980. Geology of the Otanmäki Mine. In: Häkli, T.A. (ed.), *Precambrian Ores of Finland, Guide to Excursions 078 A + C, Part 2 (Finland)*. Proceedings of the 26th International Geological Congress. Geological Survey of Finland, Espoo, pp. 25–33.
- Lukkarinen, H., 2008. Pre-Quaternary rocks of the Siilinjärvi and Kuopio map-sheet areas, Explanation to the maps of pre-Quaternary rocks, Sheets 3331 and 3242, Geological Survey of Finland, Espoo, 228 p. (in Finnish with English summary). Electronic publication available at: http://tupa.gtk.fi/kartta/kallioperakartta100/kps_3331_3242.pdf
- Lunding, E.R. & Doré, A.G., 2005. NE Atlantic break-up: a re-examination of the Iceland mantle plume model and the Atlantic–Arctic linkage. In: Doré A.G., Vining, B.A. (eds.), *Petroleum Geology: North-West Europe and Global Perspectives—Proceedings of the 6th Petroleum Geology Conference*, pp. 739–754.
<https://doi.org/10.1144/0060739>
- Marmo, V., Hoffren, V., Hytönen, K., Kallio, P., Lindholm, O. & Siivola, J., 1966. On the granites of Honkamäki and Otanmäki, Finland, with special reference to the mineralogy of accessories. *Bulletin de la Commission Géologique de Finland* 221, 34 p.
- Mattinson, J.M., 2005. Zircon U–Pb chemical abrasion (“CA-TIMS”) method: Combined annealing and multi-step partial dissolution analysis for improved precision and accuracy of zircon ages. *Chemical Geology* 220, 47–66.
<https://doi.org/10.1016/j.chemgeo.2005.03.011>
- Melezhik, V.A. & Hanski, E.J., 2013. The Pechenga greenstone belt. In: Melezhik, V.A., Prave, A.R., Hanski, E.J., Fallick, A.E., Lepland, A., Kump, L.R., Strauss, H. (eds.), *Reading the Archive of Earth’s Oxygenation. Volume 1, The Paleoproterozoic of Fennoscandia as Context for the Fennoscandian Arctic Russia – Drilling Early Earth Project*, Springer-Verlag, Berlin, Heidelberg, pp. 289–385.
https://doi.org/10.1007/978-3-642-29682-6_8
- Mikkola, P., 2011. The prehistory of Suomussalmi, eastern Finland; the first billion years as revealed by isotopes and the composition of granitoid suites. Academic Dissertation, University of Helsinki, 24 p.
- Mikkola, P., Kontinen, A., Huhma, H. & Lahaye, Y., 2010. Three Paleoproterozoic A-type granite intrusions and associated dykes from Kainuu, East Finland. *Bulletin of the Geological Society of Finland* 82, 81–100.
<https://doi.org/10.17741/bgsf/82.2.002>
- Murphy, J.B., 2007. Igneous rock associations 8. Arc magmatism II: Geochemical and isotopic characteristics. *Geoscience Canada* 34, 7–35.
- Namur, O., Charlier, B., Toplis, M.J., Higgins, M.D., Hounsell, V., Liégeois, J. & Vander Auwera, J., 2011. Differentiation of tholeiitic basalt to A-type granite in the Sept Iles layered intrusion, Canada. *Journal of Petrology* 52, 487–539.
<https://doi.org/10.1093/petrology/egq088>
- Nironen, M., 2005. Proterozoic orogenic granitoid rocks. In: Lehtinen, M., Nurmi, P. A., Rämö, O.T. (eds.), *The Precambrian Geology of Finland – Key to the Evolution of the Fennoscandian Shield*. Elsevier Science B.V., Amsterdam, pp. 443–479.
[https://doi.org/10.1016/S0166-2635\(05\)80011-8](https://doi.org/10.1016/S0166-2635(05)80011-8)
- Nykänen, V., 1995. Crystallization and chemical evolution of the lower- and central part of the Vuorokas block in the Otanmäki intrusion complex. Licentiate Thesis, University of Oulu, 135 p. (in Finnish)
- Pääkkönen, V., 1956. Otanmäki the ilmenite-magnetite ore field in Finland. *Bulletin de la Commission Géologique de Finlande* 171, 71 p.
- Pajunen, M. & Poutiainen, M., 1999. Paleoproterozoic prograde metasomatic-metamorphic overprint zones in

- Archaean tonalitic gneisses, eastern Finland. *Bulletin of the Geological Society of Finland* 71, 73–132.
<https://doi.org/10.17741/bgsf/71.1.005>
- Park, A.F., 1985. Accretion tectonism in the Proterozoic Svecofennides of the Baltic Shield. *Geology* 13, 725–729.
[https://doi.org/10.1130/0091-7613\(1985\)13<725:ATI TPS>2.0.CO;2](https://doi.org/10.1130/0091-7613(1985)13<725:ATI TPS>2.0.CO;2)
- Patiño Douce, A., 1997. Generation of metaluminous A-type granites by low pressure melting of calc-alkaline granitoids. *Geology* 25, 743–746.
[https://doi.org/10.1130/0091-7613\(1997\)025<0743:GOMATG>2.3.CO;2](https://doi.org/10.1130/0091-7613(1997)025<0743:GOMATG>2.3.CO;2)
- Pearce, J.A., 2008. Geochemical fingerprinting of oceanic basalts with applications to ophiolite classification and the search for Archean oceanic crust. *Lithos* 100, 14–48.
<https://doi.org/10.1016/j.lithos.2007.06.016>
- Pearce, J.A., Harris, N.B.W. & Tindle, A.G., 1984. Trace element discrimination diagrams for the tectonic interpretation of granitic rocks. *Journal of Petrology* 25, 956–983.
<https://doi.org/10.1093/petrology/25.4.956>
- Peltonen, P. & Kontinen, A., 2004. The Jormua ophiolite: a mafic-ultramafic complex from an ancient ocean-continent transition zone. In: Kusky, T.M. (ed.), *Precambrian Ophiolites and Related Rocks*. Elsevier B.V., Amsterdam, pp. 35–71.
[https://doi.org/10.1016/S0166-2635\(04\)13001-6](https://doi.org/10.1016/S0166-2635(04)13001-6)
- Peltonen, P., Kontinen, A. & Huhma, H., 1996. Petrology and geochemistry of metabasalts from the 1.95 Ga Jormua ophiolite, northeastern Finland. *Journal of Petrology* 37, 1359–1383.
<https://doi.org/10.1093/petrology/37.6.1359>
- Peltonen, P., Kontinen, A. & Huhma, H., 1998. Petrogenesis of the mantle sequence of the Jormua Ophiolite (Finland): Melt migration in the upper mantle during Palaeoproterozoic continental break-up. *Journal of Petrology* 39, 297–329.
<https://doi.org/10.1093/etroj/39.2.297>
- Peltonen, P., Kontinen, A., Huhma, H. & Kuronen, U., 2008. Outokumpu revisited: New mineral deposit model for the mantle peridotite-associated Cu–Co–Zn–Ni–Ag–Au sulphide deposits. *Ore Geology Reviews* 33, 559–617.
<https://doi.org/10.1016/j.oregeorev.2007.07.002>
- Perttunen, V. & Vaasjoki, M., 2001. U–Pb geochronology of the Peräpohja Schist Belt, northwestern Finland. In: Vaasjoki, M. (ed.), *Radiometric Age Determinations from Finnish Lapland and Their Bearing on the Timing of Precambrian Volcano-Sedimentary Sequences*. Geological Survey of Finland, Special Paper 33, 45–84.
- Rämö, O.T., 1991. Petrogenesis of the Proterozoic rapakivi granites and related basic rocks of southeastern Fennoscandia: Nd and Pb isotopic and general geochemical constraints. *Geological Survey of Finland, Bulletin* 355, 161 p.
- Rämö, O.T. & Haapala, I., 2005. Rapakivi granites. In: Lehtinen, M., Nurmi, P.A., Rämö, O.T. (eds.), *Precambrian Geology of Finland Key to the Evolution of the Fennoscandian Shield*. Elsevier Science B.V., Amsterdam, pp. 533–562.
[https://doi.org/10.1016/S0166-2635\(05\)80013-1](https://doi.org/10.1016/S0166-2635(05)80013-1)
- Ranta, J.-P., Lauri, L., Hanski, E., Huhma, H., Lahaye, Y. & Vanhanen, E., 2015. U–Pb and Sm–Nd isotopic constraints on the evolution of the Paleoproterozoic Peräpohja Belt, northern Finland. *Precambrian Research* 266, 246–259.
<https://doi.org/10.1016/j.precamres.2015.05.018>
- Rasilainen, K., Lahtinen, R. & Bornhorst, T.J., 2007. The Rock Geochemical Database of Finland Manual. Geological Survey of Finland, Report of Investigation 164, 38 p.
- Roberts, D.G., Thompson, M., Mitchener, B., Hossack, J., Carmichael, S. & Bjørnseth, H.M., 1999. Palaeozoic to Tertiary rift and basin dynamics: mid-Norway to the Bay of Biscay – a new context for hydrocarbon prospectivity in the deep water frontier. In: Fleet, A.J., Boldy, S.A.R. (eds.), *Petroleum Geology of Northwest Europe. Proceedings of the 5th Conference*. Geological Society London, pp. 7–40.
<https://doi.org/10.1144/0050007>
- Rudnick, R.L. & Gao, S., 2003. Composition of the continental crust. In: Rudnick, R.L. (ed.), *The Crust. Treatise on Geochemistry, Volume 3*. Elsevier-Pergamon, Oxford, pp. 1–64.
<https://doi.org/10.1016/B0-08-043751-6/03016-4>
- Sarapää, O., Kärkkäinen, N., Ahtola, T. & Al-Ani, T., 2015. High-tech metals in Finland. In: Maier, W. D., Lahtinen, R., O'Brien, H. (eds.), *Mineral Deposits of Finland*. Elsevier, Amsterdam, pp. 613–632.
<https://doi.org/10.1016/B978-0-12-410438-9.00023-6>
- Scailliet, B., Holtz, F. & Pichavant, M., 2016. Experimental constraints on the formation of silicic magmas. *Elements* 12, 109–114.
<https://doi.org/10.2113/gselements.12.2.109>
- Shellnut, J.G. & Zhou, M-F., 2007. Permian peralkaline, peraluminous and metaluminous A-type granites in the Panxi district, SW China: Their relationship to the Emeishan mantle plume. *Chemical Geology* 243, 286–316.
<https://doi.org/10.1016/j.chemgeo.2007.05.022>
- Shellnut, J.G., Zhou, M.-F. & Zellmer, G.F., 2009. The role of Fe–Ti oxide crystallization in the formation of A-type granitoids with implications for the Daly gap: An example from the Permian Baima igneous complex, SW China. *Chemical Geology* 259, 204–217.
<https://doi.org/10.1016/j.chemgeo.2008.10.044>
- Smith, D.R., Noble, J., Wobus, R.A., Unruh, D., Douglass, J., Beane, R., Davis, C., Goldman, S., Kay, G., Gustavson, B., Saltoun, B. & Stewart, J., 1999. Petrology and geochemistry of late-stage intrusions of the A-type, mid-Proterozoic Pikes Peak batholith (Central Colorado, USA): implications for petrogenetic models. *Precambrian Research* 98, 271–305.
[https://doi.org/10.1016/S0301-9268\(99\)00049-2](https://doi.org/10.1016/S0301-9268(99)00049-2)

- Streckeisen, A., 1976. To each plutonic rock its proper name. *Earth-Science Reviews* 12, 1–33.
[https://doi.org/10.1016/0012-8252\(76\)90052-0](https://doi.org/10.1016/0012-8252(76)90052-0)
- Sun, S.-S. & McDonough, W.F., 1989. Chemical and isotopic systematics of oceanic basalts; implications for mantle composition and processes. In: Saunders, A.D., Norry, M.J. (eds.), *Magmatism in the Ocean Basins*. Geological Society of London 42, 313–345.
<https://doi.org/10.1144/GSL.SP.1989.042.01.19>
- Tommasini, S., Poli, G., Manetti, P. & Conticelli, S., 1994. Oligo-Miocene A-type granites and granophyres from Yemen: isotopic and trace element constraints bearing on their genesis. *European Journal of Mineralogy* 6, 571–590.
- Tuisku, P., 1997. An introduction to Paleoproterozoic (Svecofennian) regional metamorphism in Kainuu and Lapland, Finland. In: Evins, P., Laajoki, K. (eds.), *Archaeo and Early Proterozoic (Karelian) Evolution of the Kainuu-Peräpohja Area, Northern Finland*. *Res Terrae* 13, 27–31.
- Tuisku, P. & Laajoki, K., 1990. Metamorphic and structural evolution of the Early Proterozoic Puolankajärvi Formation, Finland – II. The pressure-temperature-deformation-composition path. *Journal of Metamorphic Geology* 8, 375–391.
<https://doi.org/10.1111/j.1525-1314.1990.tb00479.x>
- Turner, S.P., Foden, J.D. & Morrison, R.S., 1992. Derivation of some A-type magmas by fractionation of basaltic magma: an example from the Padthaway Ridge, south Australia. *Lithos* 28, 151–179.
[https://doi.org/10.1016/0024-4937\(92\)90029-X](https://doi.org/10.1016/0024-4937(92)90029-X)
- Vaasjoki, M., Kärki, A. & Laajoki, K., 2001. Timing of Paleoproterozoic crustal shearing in the central Fennoscandian Shield according to U-Pb data from associated granitoids, Finland. *Bulletin of the Geological Society of Finland* 73, 87–101.
<https://doi.org/10.17741/bgsf/73.1-2.007>
- Vuollo, J. & Huhma, H., 2005. Paleoproterozoic mafic dykes in NE Finland. In: Lehtinen, M., Nurmi, P. A., Rämö, O.T. (eds.), *Precambrian Geology of Finland – Key to the Evolution of the Fennoscandian Shield*. Elsevier Science B.V., Amsterdam, pp. 193–235.
[https://doi.org/10.1016/S0166-2635\(05\)80006-4](https://doi.org/10.1016/S0166-2635(05)80006-4)
- Watson, B.E. & Harrison, M.T., 1983. Zircon saturation revisited: temperature and composition effects in a variety of crustal magma types. *Earth and Planetary Science Letters* 64, 295–304.
[https://doi.org/10.1016/0012-821X\(83\)90211-X](https://doi.org/10.1016/0012-821X(83)90211-X)
- Whalen, J.B., Currie, K.L. & Chappell, B.W., 1987. A-type granites: geochemical characteristics, discrimination and petrogenesis. *Contributions to Mineralogy and Petrology* 95, 407–419.
<https://doi.org/10.1007/BF00402202>
- Zozulya, D.R., Bayanova, T.B. & Eby, G.N., 2005. Geology and Age of the Late Archean Keivy Alkaline Province, Northeastern Baltic Shield. *Journal of Geology* 113, 601–608.
<https://doi.org/10.1086/431912>